

Thermal Activation of Hydrocarbon C–H Bonds Initiated by a Tungsten Allyl Complex

Stephen H. K. Ng, Craig S. Adams, Trevor W. Hayton, Peter Legzdins,* and Brian O. Patrick

Contribution from the Department of Chemistry, University of British Columbia, Vancouver, British Columbia, Canada V6T 1Z1

Received July 4, 2003; E-mail: legzdins@chem.ubc.ca

Abstract: Gentle thermolysis of the allyl complex, $\text{Cp}^*\text{W}(\text{NO})(\text{CH}_2\text{CMe}_3)(\eta^3\text{-H}_2\text{CCHCMe}_2)$ (**1**), at 50 °C in neat hydrocarbon solutions results in the loss of neopentane and the generation of transient intermediates that subsequently activate solvent C–H bonds. Thus, thermal reactions of **1** with tetramethylsilane, mesitylene, and benzene effect single C–H activations and lead to the exclusive formation of $\text{Cp}^*\text{W}(\text{NO})(\text{CH}_2\text{SiMe}_3)(\eta^3\text{-H}_2\text{CCHCMe}_2)$ (**2**), $\text{Cp}^*\text{W}(\text{NO})(\text{CH}_2\text{C}_6\text{H}_3\text{-3,5-Me}_2)(\eta^3\text{-H}_2\text{CCHCMe}_2)$ (**3**), and $\text{Cp}^*\text{W}(\text{NO})(\text{C}_6\text{H}_5)(\eta^3\text{-H}_2\text{CCHCMe}_2)$ (**4**), respectively. The products of reactions of **1** with other methyl-substituted arenes indicate an inherent preference of the system for the activation of stronger arene sp^2 C–H bonds. For example, C–H bond activation of *p*-xylene leads to the formation of $\text{Cp}^*\text{W}(\text{NO})(\text{CH}_2\text{C}_6\text{H}_4\text{-4-Me})(\eta^3\text{-H}_2\text{CCHCMe}_2)$ (**5**) (26%) and $\text{Cp}^*\text{W}(\text{NO})(\text{C}_6\text{H}_3\text{-2,5-Me}_2)(\eta^3\text{-H}_2\text{CCHCMe}_2)$ (**6**) (74%). Mechanistic and labeling studies indicate that the transient C–H-activating intermediates are the allene complex, $\text{Cp}^*\text{W}(\text{NO})(\eta^2\text{-H}_2\text{C}=\text{C}=\text{CMe}_2)$ (**A**), and the η^2 -diene complex, $\text{Cp}^*\text{W}(\text{NO})(\eta^2\text{-H}_2\text{C}=\text{CHC}(\text{Me})=\text{CH}_2)$ (**B**). Intermediates **A** and **B** react with cyclohexene to form $\text{Cp}^*\text{W}(\text{NO})(\eta^3\text{-CH}_2\text{C}(2\text{-cyclohexenyl})\text{CMe}_2)(\text{H})$ (**18**) and $\text{Cp}^*\text{W}(\text{NO})(\eta^3\text{-CH}_2\text{CHC}(\text{Me})\text{CH}_2\text{C}_6\text{H}_5)(\text{H})$ (**19**), respectively, and intermediate **A** can be isolated as its PMe_3 adduct, $\text{Cp}^*\text{W}(\text{NO})(\text{PMe}_3)(\eta^2\text{-H}_2\text{C}=\text{C}=\text{CMe}_2)$ (**20**). Interestingly, thermal reaction of **1** with 2,3-dimethylbut-2-ene results in the formation of a species that undergoes $\eta^3 \rightarrow \eta^1$ isomerization of the dimethylallyl ligand following the initial C–H bond-activating step to yield $\text{Cp}^*\text{W}(\text{NO})(\eta^3\text{-CMe}_2\text{CMeCH}_2)(\eta^1\text{-CH}_2\text{CHCMe}_2)$ (**21**). Thermolyses of **1** in alkane solvents afford allyl hydride complexes resulting from three successive C–H bond-activation reactions. For instance, **1** in cyclohexane converts to $\text{Cp}^*\text{W}(\text{NO})(\eta^3\text{-C}_6\text{H}_9)(\text{H})$ (**22**) with dimethylpropylcyclohexane being formed as a byproduct, and in methylcyclohexane it forms the two isomeric complexes, $\text{Cp}^*\text{W}(\text{NO})(\eta^3\text{-C}_7\text{H}_{11})(\text{H})$ (**23a,b**). All new complexes have been characterized by conventional spectroscopic methods, and the solid-state molecular structures of **2**, **3**, **4**, **18**, **19**, **20**, and **21** have been established by X-ray crystallographic analyses.

Introduction

Interest in C–H bond activations at transition-metal centers continues unabated because these processes hold the promise of leading to efficient and catalytic methods for the selective conversion of hydrocarbon feedstocks into functionalized organic compounds.¹ Considerable progress in this regard has been made in the past 20 years, and numerous metal-containing complexes have been discovered to effect intermolecular C–H bond activations, often selectively and under relatively mild conditions.² Notable examples include (1) late transition-metal complexes that oxidatively add C–H linkages to the metal center, (2) transition-metal, lanthanide, and actinide complexes that facilitate C–H activation via M–C σ -bond metathesis, and (3) early- to mid-transition-metal complexes that add C–H bonds across M=N and M=C linkages. A fundamental understanding of the discrete C–H activation processes has been acquired for many of these complexes, and the chemistry of

select systems has been significantly advanced toward efficient, catalytic functionalizations.²

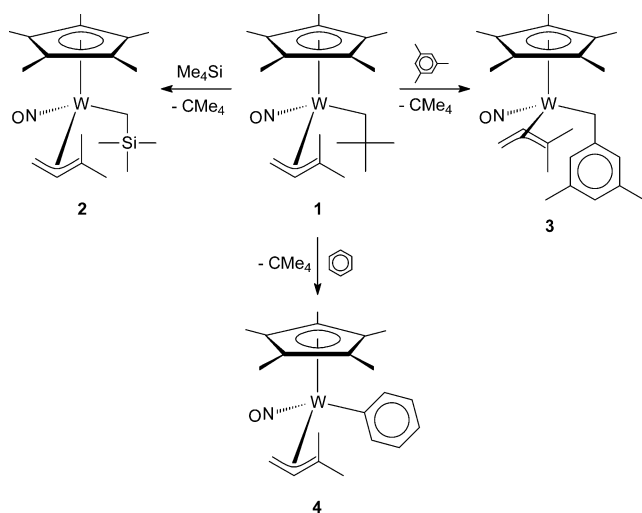
Our contributions to this area of chemistry began with our recent discovery that $\text{Cp}^*\text{M}(\text{NO})(\text{hydrocarbyl})_2$ complexes ($\text{Cp}^* = \eta^5\text{-C}_5\text{Me}_5$) of molybdenum and tungsten exhibit hydrocarbyl-dependent thermal chemistry.³ Thus, gentle thermolysis of appropriate $\text{Cp}^*\text{M}(\text{NO})(\text{hydrocarbyl})_2$ precursors ($\text{M} = \text{Mo}, \text{W}$) results in loss of hydrocarbon and the transient formation of 16-electron organometallic complexes such as $\text{Cp}^*\text{M}(\text{NO})(\text{alkylidene})$, $\text{Cp}^*\text{M}(\text{NO})(\eta^2\text{-acetylene})$, and $\text{Cp}^*\text{M}(\text{NO})(\eta^2\text{-benzyne})$. These intermediates first effect the single activation of hydrocarbon C–H bonds intermolecularly via the reverse of the transformations by which they were generated. Some of the new product complexes formed in this manner are stable and may be isolated. Others are thermally unstable under the experimental conditions employed and react further to effect double or triple C–H bond activations of the hydrocarbon substrates. We now report the thermal chemistry of the related

(1) Crabtree, R. H. *J. Chem. Soc., Dalton Trans.* **2001**, 2437.

(2) Labinger, J. A.; Bercaw, J. E. *Nature* **2002**, 417, 507 and references therein.

(3) Pamplin, C. B.; Legzdins, P. *Acc. Chem. Res.* **2003**, 36, 223.

Scheme 1



tungsten allyl complex, $\text{Cp}^*\text{W}(\text{NO})(\text{CH}_2\text{CMe}_3)(\eta^3\text{-H}_2\text{CCHCMe}_2)$ (**1**), which loses neopentane at 50 °C and forms an allene complex and an η^2 -diene complex as reactive intermediates. Both of these intermediates effect a variety of hydrocarbon C–H bond activations, some of which are without precedent in the chemical literature. To the best of our knowledge, this work constitutes the first confirmed examples of metal-allene and metal-diene species functioning in this manner. A portion of this work has been communicated previously.⁴

Results and Discussion

Single C–H Bond Activations Initiated by 1. (A) Activation of Tetramethylsilane, Mesitylene, and Benzene. Scheme 1 summarizes the C–H bond activations discovered during the course of this study that afford one principal organometallic product following exclusive reaction with a single C–H bond of the hydrocarbon substrate.

Thermolysis of **1** in neat tetramethylsilane at 50 °C for 6 h results in the quantitative formation of the alkyl-allyl complex, $\text{Cp}^*\text{W}(\text{NO})(\text{CH}_2\text{SiMe}_3)(\eta^3\text{-H}_2\text{CCHCMe}_2)$ (**2**). Complex **2** is thermally stable in tetramethylsilane under these conditions, and the known bis(alkyl) complex, $\text{Cp}^*\text{W}(\text{NO})(\text{CH}_2\text{SiMe}_3)_2$, is not formed on prolonged reaction times. A single-crystal X-ray crystallographic analysis has been performed on **2**, and the resulting ORTEP diagram is shown in Figure 1. The solid-state molecular structure of **2** exhibits a strong σ – π distortion of the dimethylallyl ligand as evidenced by its long C(11)–C(12) (1.46(1) Å) and short C(12)–C(13) (1.348(9) Å) linkages, suggestive of more single- and double-bond character, respectively.⁵ NMR data indicate that this distortion persists in solutions. Thus, the $^{13}\text{C}\{^1\text{H}\}$ NMR spectrum of **2** in C_6D_6 exhibits a resonance at 101.9 ppm (allyl-CH) characteristic of an sp^2 -like carbon and a signal at 39.3 ppm (allyl- CH_2) indicative of an sp^3 -like terminal carbon. Other chiral transition-metal allyl complexes display similar spectroscopic and solid-state properties that are reflective of σ – π distortions of this type.^{6–9}

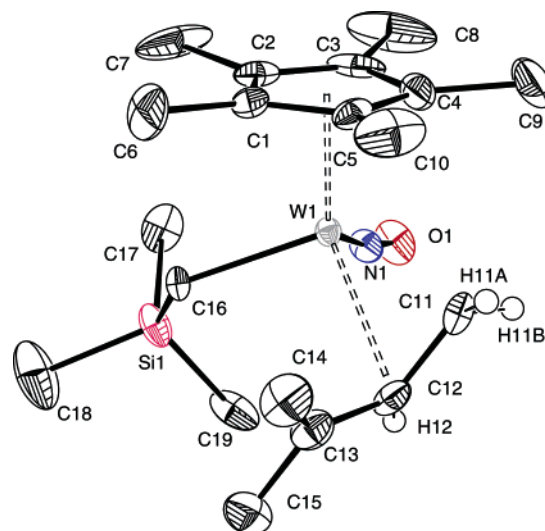


Figure 1. Solid-state molecular structure of $\text{Cp}^*\text{W}(\text{NO})(\text{CH}_2\text{SiMe}_3)(\eta^3\text{-H}_2\text{CCHCMe}_2)$ (**2**) with 50% probability thermal ellipsoids shown. Selected interatomic distances (Å) and angles (deg): W1–N1 = 1.760(5), W1–C11 = 2.182(6), W1–C12 = 2.433(6), W1–C13 = 2.874(6), W1–C16 = 2.217(6), C11–C12 = 1.46(1), C12–C13 = 1.348(9), N1–O1 = 1.237(7), W1–N1–O1 = 170.7(5), C11–C12–C13 = 124.9(7), W1–C11–C12 = 81.2(4), C12–C13–C14 = 125.6(7), C14–C13–C15 = 113.5(7).

The dimethylallyl ligand in **2** adopts an endo configuration in the solid state (Figure 1). This configuration is identical to that extant in its solution structure as determined by selective NOE NMR spectroscopic data¹⁰ and is probably a manifestation of minimization of the intramolecular steric interactions between the methyls on the allyl ligand and the rapidly rotating methyl groups of the trimethylsilylmethyl ligand. Another interesting feature is the orientation of the dimethylallyl ligand so that the most substituted carbon atom of its three-carbon allyl backbone, that is, C(13), is situated trans to the NO ligand. This orientation can be attributed to the electronic asymmetry at the tungsten center resulting from the different acceptor characteristics of the NO and the alkyl ligands.¹¹ This electronic asymmetry also results in markedly different W–C(allyl) distances which range from 2.182(6) Å for W–C(11) to 2.874(6) Å for W–C(13) in **2**. Finally, the substituted allyl ligand is also oriented so as to maximize the π -interaction between the nonbonding orbital of the allyl ligand and the metal center.¹²

The thermal reaction of **1** in mesitylene results only in the formation of $\text{Cp}^*\text{W}(\text{NO})(\text{CH}_2\text{C}_6\text{H}_3\text{-3,5-Me}_2)(\eta^3\text{-H}_2\text{CCHCMe}_2)$ (**3**) (Scheme 1). The exclusive activation of benzylic sp^3 C–H bonds during this transformation is similar to the behavior exhibited by other previously studied $\text{Cp}^*\text{W}(\text{NO})$ -containing

(4) Ng, S. H. K.; Adams, C. S.; Legzdins, P. *J. Am. Chem. Soc.* **2002**, *124*, 9380.

(5) Bent, H. A. *Chem. Rev.* **1961**, *61*, 275.

(6) Ipaktschi, J.; Mirzaei, F.; Demuth-Eberle, G. J.; Beck, J.; Serafin, M. *Organometallics* **1997**, *16*, 3965.

(7) Frohnapfel, D. S.; White, P. S.; Templeton, J. L. *Organometallics* **1997**, *16*, 3737.

(8) Villanueva, L. A.; Ward, Y. D.; Lachicotte, R.; Liebeskind, L. S. *Organometallics* **1996**, *15*, 4190.

(9) Adams, R. D.; Chodosh, D. F.; Faller, J. W.; Rosan, A. M. *J. Am. Chem. Soc.* **1979**, *101*, 2570.

(10) Direct evidence for *endo*- versus *exo*-allyl conformations using selective NOE NMR spectroscopy is sometimes not available, and logical inferences must be made to ascertain the solution structure. For example, irradiation of the signal due to the central allyl H atom leading to an NOE enhancement of the Cp^* methyl H atoms signal is direct evidence for an *exo* configuration. However, its absence, and hence the implication of an *endo* configuration, must be confirmed by irradiation of the trans Me group signal that should exhibit an NOE enhancement of the Cp^* ring signal.

(11) Faller, J. W.; DiVerdi, M. J.; John, J. A. *Tetrahedron Lett.* **1991**, *32*, 1271.

(12) Schilling, B. E. R.; Hoffman, R.; Faller, J. W. *J. Am. Chem. Soc.* **1979**, *101*, 592.

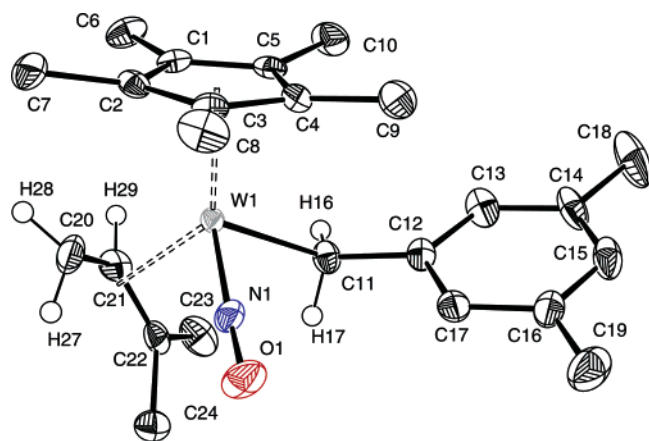


Figure 2. Solid-state molecular structure of $\text{Cp}^*\text{W}(\text{NO})(\text{CH}_2\text{C}_6\text{H}_3\text{-3,5-Me}_2)(\eta^3\text{-H}_2\text{CCHCMe}_2)$ (**3**) with 50% probability thermal ellipsoids shown. Selected interatomic distances (Å) and angles (deg): $\text{W1-N1} = 1.753(4)$, $\text{W1-C20} = 2.187(5)$, $\text{W1-C21} = 2.391(5)$, $\text{W1-C22} = 2.961(5)$, $\text{W1-C11} = 2.239(4)$, $\text{N1-O1} = 1.240(5)$, $\text{C20-C21} = 1.454(8)$, $\text{C21-C22} = 1.365(6)$, $\text{C11-C12} = 1.493(6)$, $\text{W1-N1-O1} = 171.1(4)$, $\text{W1-C20-C21} = 79.3(3)$, $\text{W1-C11-C12} = 120.5(3)$, $\text{C20-C21-C22} = 125.5(5)$, $\text{C21-C22-C24} = 123.5(4)$, $\text{C23-C22-C24} = 115.2(4)$.

systems,¹³ and it is a result of the mesitylene methyl groups hindering access of the tungsten center to the arene's sp^2 C–H bonds. The ORTEP diagram of the solid-state molecular structure of **3** is shown in Figure 2.

The exo conformation adopted by the dimethylallyl ligand in **3** in the solid state is consistent with its apparent solution structure as deduced from selective NOE NMR spectroscopic data.¹⁰ This conformation is in contrast to the endo configuration observed in solution for complex **1** and the solution- and solid-state molecular structures of **2**. Theoretical calculations performed on similar asymmetric allyl transition-metal complexes reveal that there is a minimal energy difference between the idealized endo and exo conformers,¹² thus suggesting that the two different orientations observed for complexes **1**, **2**, and **3** are the result of intramolecular steric factors operative in the various molecules. As outlined for **2** (vide supra), the solid-state molecular structure of **3** (Figure 2) also exhibits the customary intramolecular metrical parameters reflective of the electronic asymmetry existing at the metal center. Indeed, these features are common to all of the chiral allyl nitrosyl complexes characterized structurally during this work.

The thermal reaction of **1** in benzene affords exclusively the phenyl dimethylallyl product, $\text{Cp}^*\text{W}(\text{NO})(\text{C}_6\text{H}_5)(\eta^3\text{-H}_2\text{CCHCMe}_2)$ (**4**) (Scheme 1). A single-crystal X-ray crystallographic analysis has been performed to confirm the identity of the final organometallic product, and the ORTEP diagram of **4** is shown in Figure 3. Not surprisingly, the interatomic distances and angles of **4** are comparable to those extant in the solid-state molecular structures of **2** and **3**.

(B) Activations of Xylenes and Toluene. The thermal reaction of **1** in *p*-xylene at 50 °C results in the formation of two organometallic products in essentially quantitative yields (eq 1). The product generated upon activation of a benzylic sp^3 C–H bond of *p*-xylene, $\text{Cp}^*\text{W}(\text{NO})(\text{CH}_2\text{C}_6\text{H}_4\text{-4-Me})(\eta^3\text{-H}_2\text{CCHCMe}_2)$ (**5**), and that from the activation of an aromatic sp^2 C–H bond, $\text{Cp}^*\text{W}(\text{NO})(\text{C}_6\text{H}_3\text{-2,5-Me}_2)(\eta^3\text{-H}_2\text{CCHCMe}_2)$ (**6**),¹⁴

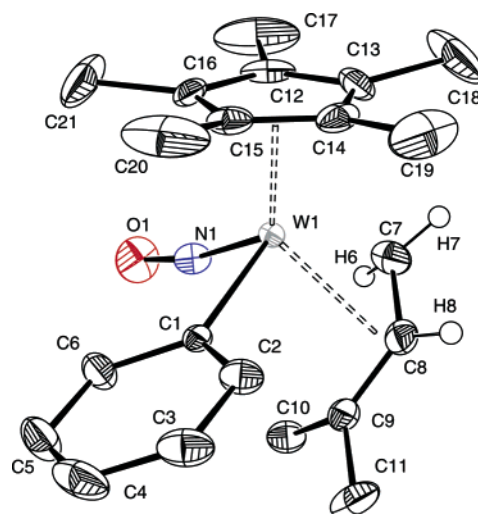
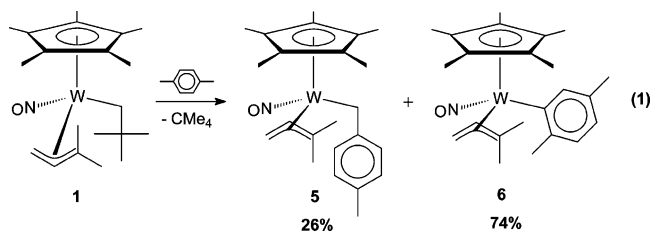


Figure 3. Solid-state molecular structure of $\text{Cp}^*\text{W}(\text{NO})(\text{C}_6\text{H}_5)(\eta^3\text{-H}_2\text{CCHCMe}_2)$ (**4**) with 50% probability thermal ellipsoids shown. Selected interatomic distances (Å) and angles (deg): $\text{W1-N1} = 1.762(3)$, $\text{W1-C7} = 2.218(4)$, $\text{W1-C8} = 2.363(4)$, $\text{W1-C9} = 2.768(4)$, $\text{W1-C1} = 2.186(3)$, $\text{N1-O1} = 1.224(4)$, $\text{C7-C8} = 1.439(6)$, $\text{C8-C9} = 1.365(5)$, $\text{W1-N1-O1} = 169.5(3)$, $\text{W1-C1-C6} = 121.4(2)$, $\text{C7-C8-C9} = 124.8(4)$, $\text{W1-C7-C8} = 77.3(2)$, $\text{C8-C9-C10} = 124.3(4)$, $\text{C10-C9-C11} = 113.5(3)$.

are formed in an approximate 1:3 ratio which persists even after 3 times the normal reaction time of 6 h. The distribution of products indicates a tendency of this system to preferentially



activate aromatic C–H bonds over benzylic ones, a trend commonly seen with many C–H-activating transition-metal complexes.¹³ The customary rationalization of this selectivity involves the thermodynamics of the bond-breaking and bond-forming steps. Although the bond-dissociation energy for an sp^2 C–H bond is greater than that for an sp^3 C–H bond, the resulting metal–carbon interaction is stronger for a $\text{M-C}(\text{sp}^2)$ linkage than for a $\text{M-C}(\text{sp}^3)$ bond.^{15–19}

The thermolyses of **1** in *m*- or *o*-xylene result in similar transformations. The thermal reaction with *m*-xylene affords three products, $\text{Cp}^*\text{W}(\text{NO})(\text{CH}_2\text{C}_6\text{H}_4\text{-3-Me})(\eta^3\text{-H}_2\text{CCHCMe}_2)$ (**7**), $\text{Cp}^*\text{W}(\text{NO})(\text{C}_6\text{H}_3\text{-2,4-Me}_2)(\eta^3\text{-H}_2\text{CCHCMe}_2)$ (**8**), and $\text{Cp}^*\text{W}(\text{NO})(\text{C}_6\text{H}_3\text{-3,5-Me}_2)(\eta^3\text{-H}_2\text{CCHCMe}_2)$ (**9**) (eq 2). Not surprisingly, the ratio of the final products is comparable to that observed for the benzylic- and aromatic-activated complexes **5** and **6** (see eq 1).

(14) A single-crystal X-ray crystallographic analysis of **6** has been performed. Its solid-state structural features are similar to those exhibited by other *p*-xylene aryl C–H-activated tungsten nitrosyl complexes.

(15) Johansson, L.; Ryan, O. B.; Romming, C.; Tilset, M. *J. Am. Chem. Soc.* **2001**, *123*, 6579.

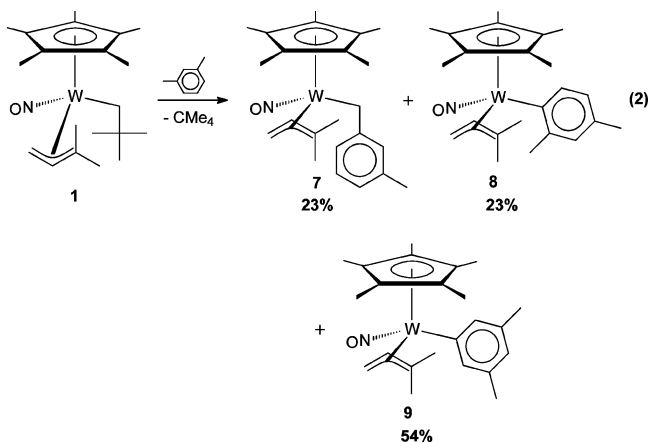
(16) Bryndza, H. E.; Fong, L. K.; Paciello, R. A.; Tam, W.; Bercaw, J. E. *J. Am. Chem. Soc.* **1987**, *109*, 1444.

(17) Jones, W. D.; Hessel, E. T. *J. Am. Chem. Soc.* **1993**, *115*, 554.

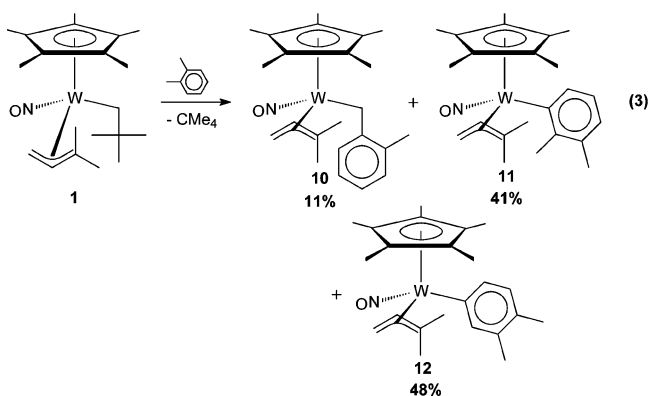
(18) Jones, W. D.; Feher, F. J. *Acc. Chem. Res.* **1989**, *22*, 91.

(19) Jones, W. D.; Feher, F. J. *J. Am. Chem. Soc.* **1984**, *106*, 1650.

(13) Adams, C. S.; Legzdins, P.; Tran, E. *Organometallics* **2002**, *21*, 1474.



The thermal reaction of **1** with *o*-xylene also affords three organometallic products, $\text{Cp}^*\text{W}(\text{NO})(\text{CH}_2\text{C}_6\text{H}_4\text{-2-Me})(\eta^3\text{-H}_2\text{CCHCMe}_2)$ (**10**), $\text{Cp}^*\text{W}(\text{NO})(\text{C}_6\text{H}_3\text{-2,3-Me}_2)(\eta^3\text{-H}_2\text{CCHCMe}_2)$ (**11**), and $\text{Cp}^*\text{W}(\text{NO})(\text{C}_6\text{H}_3\text{-3,4-Me}_2)(\eta^3\text{-H}_2\text{CCHCMe}_2)$ (**12**) (eq 3).

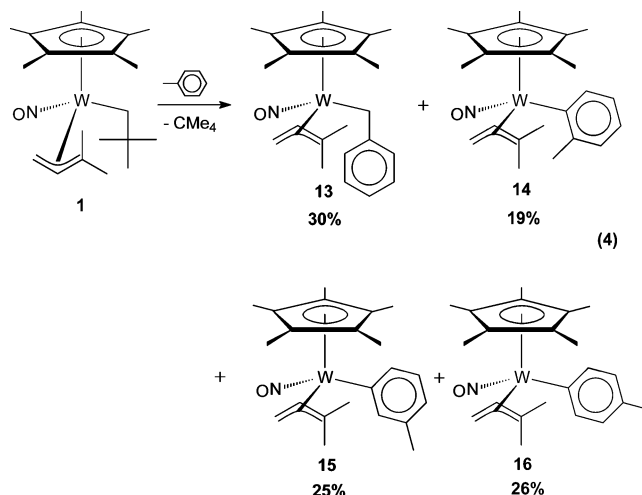


The most striking feature of the product ratios obtained with *o*-xylene is the markedly decreased proportion of the benzylic C–H-activated species **10**. This trend of decreasing benzylic C–H activation in different xylene solvents (i.e., para > meta > ortho) is similar to that seen for the related $\text{Cp}^*\text{W}(\text{NO})$ -(alkylidene) complexes.¹³ This feature is probably a manifestation of the steric hindrance imposed on the sp^3 C–H bonds by the adjacent methyl group in *o*-xylene and less overall hindrance of the sp^2 C–H bonds, both factors subsequently increasing the preference for the formation of the aromatic-activated complexes.

The thermolysis of **1** in toluene leads to the formation of all four products of single C–H bond activation, $\text{Cp}^*\text{W}(\text{NO})(\text{CH}_2\text{C}_6\text{H}_5)(\eta^3\text{-H}_2\text{CCHCMe}_2)$ (**13**), $\text{Cp}^*\text{W}(\text{NO})(\text{C}_6\text{H}_4\text{-2-Me})(\eta^3\text{-H}_2\text{CCHCMe}_2)$ (**14**), $\text{Cp}^*\text{W}(\text{NO})(\text{C}_6\text{H}_4\text{-3-Me})(\eta^3\text{-H}_2\text{CCHCMe}_2)$ (**15**), and $\text{Cp}^*\text{W}(\text{NO})(\text{C}_6\text{H}_4\text{-4-Me})(\eta^3\text{-H}_2\text{CCHCMe}_2)$ (**16**) (eq 4). Complexes **14–16** were characterized as a mixture by ^1H NMR spectroscopy, and thus many of the resonances expected for each individual compound were not discernible due to overlapping signals.

Again, the product ratios observed for complexes **13–16** are invariant with time, and the proportion of aryl:benzyl species (i.e., 70:30) is similar to those observed for products from activation of the various C–H bonds of *m*- and *p*-xylene (vide supra). We have also established by independent NMR experi-

ments that the pure benzyl products of conversions 1–4 do not convert to the aryl products under the experimental conditions employed. Consistently, the isolated aryl products also do not convert to the benzyl products. However, we have been unable to isolate any one of the individual aryl products to determine whether it interconverts with its aryl isomers. All attempts at isolation afford a mixture of aryl products in the proportions specified in eqs 1–4.



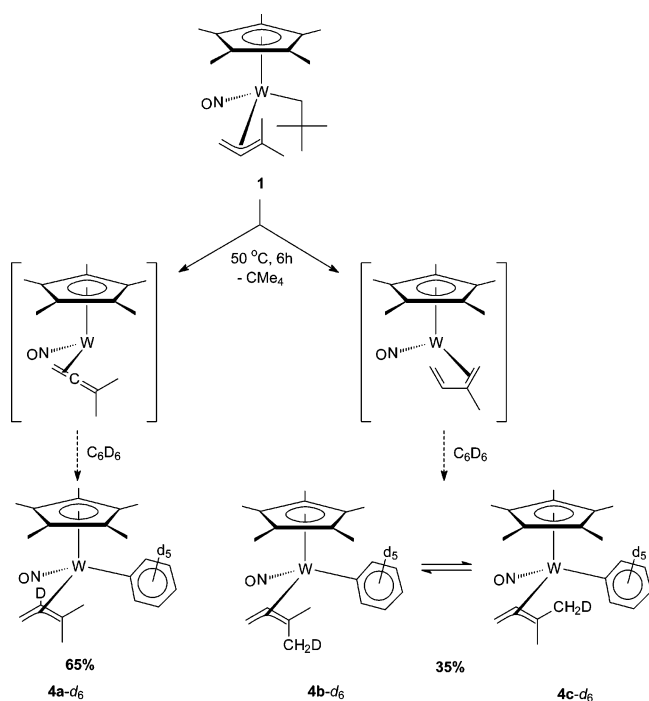
Mechanistic Investigations of Single C–H Bond Activations Initiated by 1. The thermolysis of **1** in benzene- d_6 at 50 °C (the temperature employed throughout these studies) results in the elimination of neopentane and the formation of several new organometallic complexes, the isomeric $\text{Cp}^*\text{W}(\text{NO})(\text{C}_6\text{D}_5)(\eta^3\text{-CH}_2\text{CDCMe}_2)$ (**4a-d₆**), $\text{Cp}^*\text{W}(\text{NO})(\text{C}_6\text{D}_5)(\eta^3\text{-CH}_2\text{-CHCMe}(\text{CH}_2\text{D}))$ (**4b-d₆**), and $\text{Cp}^*\text{W}(\text{NO})(\text{C}_6\text{D}_5)(\eta^3\text{-CH}_2\text{CHC}(\text{CH}_2\text{D})\text{Me})$ (**4c-d₆**). Reactant **1** is consumed via a pseudo first-order process with an observed rate constant of $2.2(1) \times 10^{-4} \text{ s}^{-1}$ ($R^2 = 0.999$). The magnitude of this rate constant is comparable to that found for the related rate-limiting loss of neopentane from $\text{Cp}^*\text{W}(\text{NO})(\text{CH}_2\text{CMe}_3)_2$ at 70 °C.²⁰

Complexes **4a–c-d₆** have been identified from their $^2\text{H}\{^1\text{H}\}$ and ^1H NMR spectroscopic data which also provide the product ratios shown in Scheme 2. Deuterium incorporation into the dimethylallyl ligands of the final products in the manner shown suggests that reactive intermediates such as an allene or a diene complex are generated via hydrogen abstraction from the dimethylallyl ligand in **1** to form a transition-state entity that eventually eliminates neopentane. The activation of a benzene C–D bond could then proceed via the microscopic reverse processes to afford the final labeled allyl phenyl complexes. However, an independently prepared sample of the *trans*-diene complex, $\text{Cp}^*\text{W}(\text{NO})(\eta^4\text{-trans-H}_2\text{C}=\text{CHC}(\text{Me})=\text{CH}_2)$ (**17**), is unreactive in benzene- d_6 under the customary thermolysis conditions. Consequently, **17** is most likely not an intermediate involved in the formation of **4b,c-d₆**. Furthermore, no incorporation of deuterium into the Cp^* ring is evident from the $^2\text{H}\{^1\text{H}\}$ NMR spectrum of the final reaction mixture, thereby eliminating the possibility of a C–H activation pathway via oxidative addition of a tucked-in Cp^* -methyl C–H bond.²¹

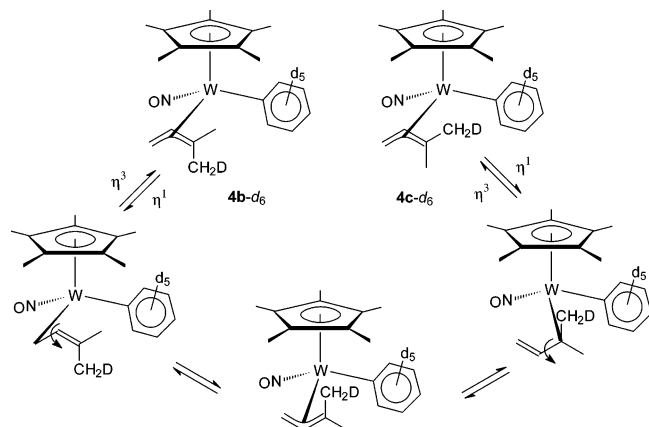
(20) Adams, C. S.; Legzdins, P.; Tran, E. *J. Am. Chem. Soc.* **2001**, *123*, 612.

(21) Schock, L. E.; Brock, C. P.; Marks, T. J. *Organometallics* **1987**, *6*, 232.

Scheme 2



Scheme 3



The incorporation of deuterium at both methyl positions of the dimethylallyl ligand can be rationalized by the mechanism shown in Scheme 3, which is supported by the room-temperature EXSY NMR spectrum of **4** in C₆D₆ that exhibits cross-peaks attributable to exchange of the methyl groups of the allyl ligand. The proposed pathway hinges on the ability of the σ - π distorted η^3 -allyl fragments to break the two-electron bond, rotate about the remaining single bond to exchange the terminal allyl substituents, and then revert back to the original η^3 -endo or -exo configuration. Such processes do have literature precedents.^{22–25}

Reaction Products Indicative of Allene and Diene Intermediates. The thermal reaction of **1** in cyclohexene leads to the formation of two allyl-containing products, Cp*W(NO)(η^3 -

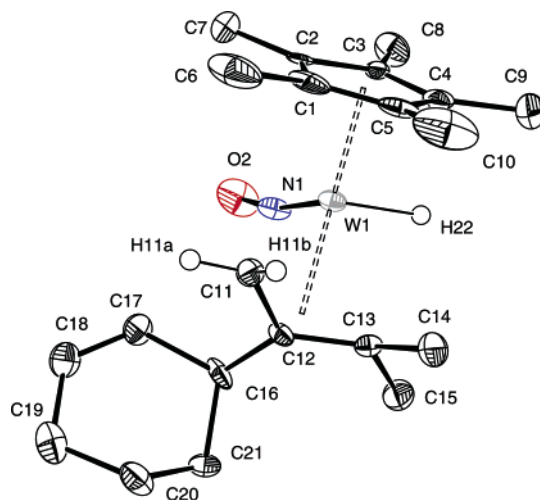


Figure 4. Solid-state molecular structure of Cp*W(NO)(η^3 -CH₂C(2-cyclohexenyl)CMe₂)(H) (**18**) with 50% probability thermal ellipsoids shown. Selected interatomic distances (Å) and angles (deg): W1–N1 = 1.774(5), W1–C11 = 2.258(5), W1–C12 = 2.333(5), W1–C13 = 2.407(5), N1–O1 = 1.227(6), C11–C12 = 1.434(7), C12–C13 = 1.405(7), C17–C18 = 1.326(7), W1–N1–O1 = 167.1(4), C11–C12–C13 = 118.7(5), C12–C13–C14 = 122.2(4).

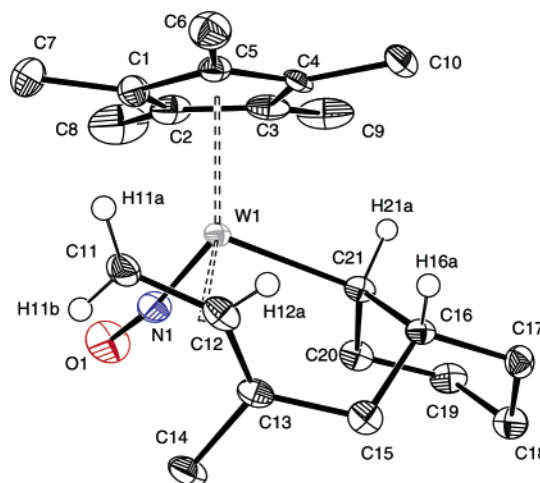
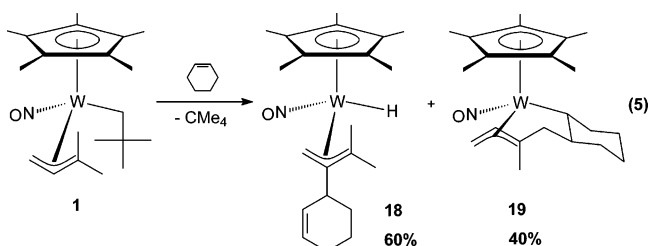


Figure 5. Solid-state molecular structure of Cp*W(NO)(η^3 -CH₂CHC(Me)-CH₂C β H(C₄H₈)C α H) (**19**) with 50% probability thermal ellipsoids shown. Selected interatomic distances (Å) and angles (deg): W1–N1 = 1.773(5), W1–C11 = 2.232(5), W1–C12 = 2.290(5), W1–C13 = 2.568(6), N1–O1 = 1.232(6), C11–C12 = 1.426(9), C12–C13 = 1.381(8), W1–N1–O1 = 170.1(5), C11–C12–C13 = 122.0(6).

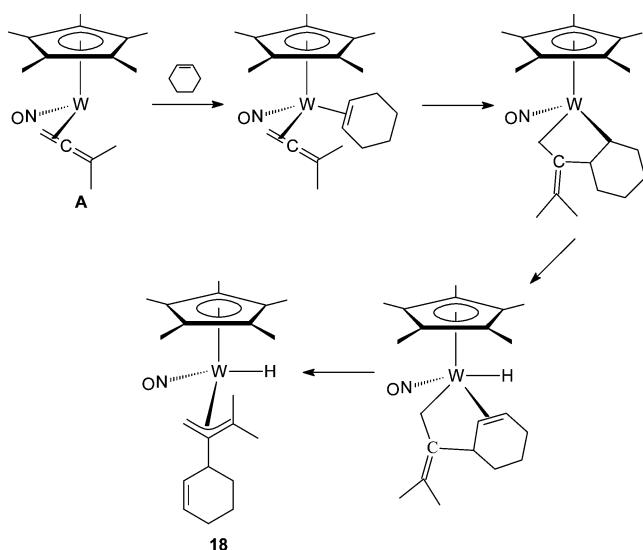
CH₂C(2-cyclohexenyl)CMe₂)(H) (**18**) and Cp*W(NO)(η^3 -CH₂-CHC)(Me)CH₂C β H(C₄H₈)C α H) (**19**) (eq 5).



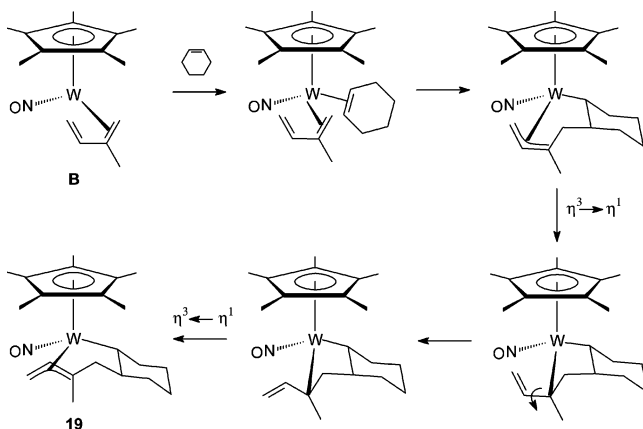
Single-crystal X-ray crystallographic analyses have been performed on **18** and **19**, and the resulting ORTEP diagrams are shown in Figures 4 and 5, respectively. Interestingly, both complexes show less pronounced structural manifestations of

- (22) Becconsall, J. K.; Job, B. E.; O'Brien, S. J. *Chem. Soc. A* **1967**, 423.
 (23) Benn, R.; Rufinska, A.; Schroth, G. J. *Organomet. Chem.* **1981**, 217, 91.
 (24) Thompson, M. E.; Baxter, S. M.; Bulls, A. R.; Burger, B. J.; Nolan, M. C.; Santarsiero, B. D.; Schaefer, W. P.; Bercaw, J. E. *J. Am. Chem. Soc.* **1987**, 109, 203.
 (25) Abrams, M. B.; Yoder, J. C.; Loeber, C.; Day, M. W.; Bercaw, J. E. *Organometallics* **1999**, 18, 1389.

Scheme 4



Scheme 5



the electronic asymmetry at their tungsten centers than do the other allyl complexes isolated during this work.

The most plausible rationale for the origin of these products involves two pathways originating at **1** that generate two different reactive intermediates, the allene complex, $\text{Cp}^*\text{W}(\text{NO})(\eta^2\text{-H}_2\text{C}=\text{C}=\text{CMe}_2)$ (**A**), and the diene complex, $\text{Cp}^*\text{W}(\text{NO})(\eta^2\text{-H}_2\text{C}=\text{CHC}(\text{Me})=\text{CH}_2)$ (**B**) (Schemes 4 and 5, respectively). This reactivity exhibited by the purported allene intermediate is not surprising, given the numerous examples in the literature of metal-mediated C–C bond coupling of allenes with other unsaturated organic species.^{26–30}

On the basis of previous studies performed on similar systems,³¹ we originally thought that **19** could also be derived from a C–C bond-coupling reaction between a *trans*-diene complex and an incoming cyclohexene molecule. However, the thermolysis of the independently synthesized *trans*-diene complex **17** in excess cyclohexene results in no reaction. This

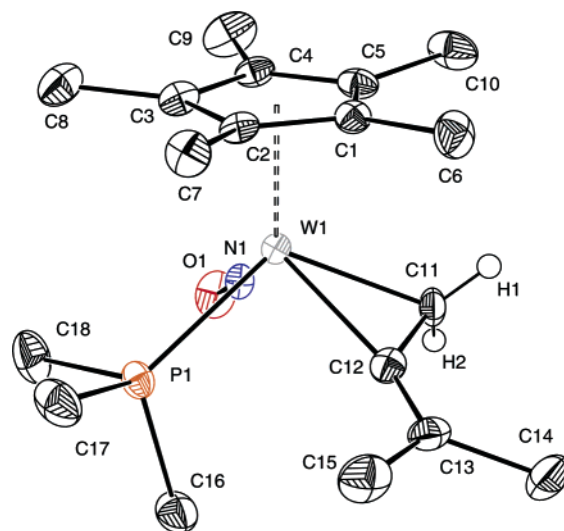
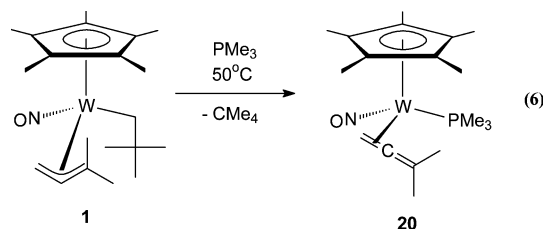


Figure 6. Solid-state molecular structure of $\text{Cp}^*\text{W}(\text{NO})(\text{PMe}_3)(\eta^2\text{-H}_2\text{C}=\text{C}=\text{CMe}_2)$ (**20**) with 50% probability thermal ellipsoids shown. Selected interatomic distances (Å) and angles (deg): $\text{W1}-\text{N1} = 1.795(4)$, $\text{W1}-\text{C11} = 2.205(4)$, $\text{W1}-\text{C12} = 2.148(5)$, $\text{W1}-\text{P1} = 2.466(12)$, $\text{N1}-\text{O1} = 1.224(5)$, $\text{C11}-\text{C12} = 1.436(7)$, $\text{C12}-\text{C13} = 1.324(7)$, $\text{W1}-\text{N1}-\text{O1} = 175.0(4)$, $\text{N1}-\text{W1}-\text{C11} = 91.00(18)$, $\text{C12}-\text{W1}-\text{C11} = 38.49(18)$, $\text{C11}-\text{C12}-\text{C13} = 134.0(5)$, $\text{C12}-\text{C13}-\text{C14} = 121.8(5)$, $\text{C12}-\text{C13}-\text{C15} = 124.3(5)$.

observation, taken in conjunction with labeling studies conducted on this system (vide supra), suggests that the two reactive intermediates, **A** and **B**, are simultaneously generated thermally from **1** via two different mechanisms, both involving intramolecular hydrogen abstraction from the dimethylallyl ligand.

Trapping of the Allene Intermediate. The thermal reaction of **1** in neat trimethylphosphine yields the base-stabilized adduct of the dimethylallene complex, $\text{Cp}^*\text{W}(\text{NO})(\text{PMe}_3)(\eta^2\text{-H}_2\text{C}=\text{C}=\text{CMe}_2)$ (**20**) (eq 6), which has been isolated in 24% yield. Interestingly, there is no evidence in the ^1H NMR spectrum of the final reaction mixture suggesting the presence of a phosphine-stabilized η^2 -diene species.



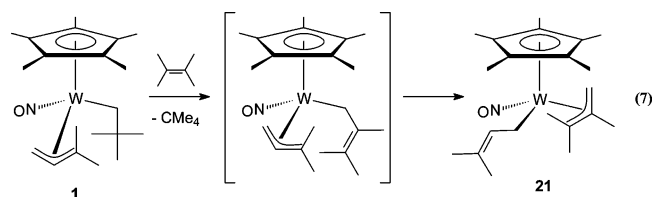
The ORTEP diagram of **20** shown in Figure 6 confirms that one of the reactive intermediates responsible for the C–H bond-activating chemistry of **1** is the η^2 -dimethylallene complex. The most notable feature of the solid-state molecular structure of **20** is the nonlinear nature of the allene ligand framework, a feature that has also been documented for other η^2 -allene complexes.^{30,32–40} The $\text{C}(11)-\text{C}(12)-\text{C}(13)$ angle of $134.0(5)^\circ$

- (26) Wu, I. Y.; Tsai, J. H.; Huang, B. C.; Chen, S. C.; Lin, Y. C. *Organometallics* **1993**, *12*, 3971.
 (27) Doxsee, K. M.; Juliette, J. J.; Zientara, K.; Nieckarz, G. *J. Am. Chem. Soc.* **1994**, *116*, 2147.
 (28) Yin, J.; Jones, W. M. *Tetrahedron* **1995**, *51*, 4395.
 (29) Murakami, M.; Itami, K.; Ito, Y. *J. Am. Chem. Soc.* **1997**, *119*, 7163.
 (30) Choi, J. C.; Sarai, S.; Koizumi, T.; Osakada, K.; Yamamoto, T. *Organometallics* **1998**, *17*, 2037.
 (31) Christensen, N. J.; Legzdins, P.; Einstein, F. W. B.; Jones, R. H. *Organometallics* **1991**, *10*, 3070.

- (32) Racanelli, P.; Pantini, G.; Immirzi, A.; Allegra, G.; Porri, L. *Chem. Commun.* **1969**, 361.
 (33) Binger, P.; Langhauser, F.; Wedeman, P.; Gabor, B.; Mynott, R.; Kruger, C. *Chem. Ber.* **1994**, *127*, 39.
 (34) Clark, H. C.; Dymarski, M. J.; Payne, N. C. *J. Organomet. Chem.* **1979**, *165*, 117.
 (35) Lentz, D.; Willemsen, S. *Organometallics* **1999**, *18*, 3962.
 (36) Werner, H.; Schneider, D.; Schulz, M. *J. Organomet. Chem.* **1993**, *451*, 175.
 (37) Pu, J.; Peng, T.-S.; Arif, A. M.; Gladysz, J. A. *Organometallics* **1992**, *11*, 3232.

is among the most acute yet found for acyclic allene complexes,⁴¹ and it is a manifestation of the considerable back-donation of electron density from the metal center to the η^2 -allene π^* orbitals. The ability of $\text{Cp}^*\text{W}(\text{NO})(\text{PR}_3)_3$ fragments to function as strong π -bases has been previously documented,⁴² and in **20** it results in the lengthening of $\text{C}(11)\text{--C}(12)$ (1.436(7) Å) relative to that in the uncoordinated dimethylallene (1.324(7) Å). This elongation suggests a decrease in the $\text{C}(11)\text{--C}(12)$ bond order from formally two to almost one. This view is further supported by evidence gathered from ^1H and $^{13}\text{C}\{^1\text{H}\}$ NMR spectroscopic data. The large upfield shifts observed for the methylene carbon (δ 7.7) and hydrogen (δ 0.67, 1.97) signals are consistent with the terminal carbon having considerable sp^3 character.⁴³ This upfield shift is also evident for the central carbon atom signal (δ 165.7), while the remaining assignable resonances are relatively unchanged from those exhibited by free dimethylallene.

Formation of an η^1 -Dimethylallyl Complex. In an attempt to obtain additional evidence supporting the existence of the diene reactive intermediate, the thermolysis of **1** was effected in 2,3-dimethyl-2-butene with the anticipation that two products would be formed that would implicate the two suggested reactive intermediates in a manner similar to that found in the reaction with cyclohexene (vide supra). However, in this instance, $\text{Cp}^*\text{W}(\text{NO})(\eta^3\text{-Me}_2\text{CCMeCH}_2)(\eta^1\text{-CH}_2\text{CHCMe}_2)$ (**21**) is formed exclusively (eq 7). A single-crystal X-ray crystallographic analysis has been performed to ascertain the connectivity of the atoms in this organometallic complex, and the resulting ORTEP diagram of **21** is shown in Figure 7. This alternate allyl complex presumably results from the activation of a methyl C–H bond of 2,3-dimethyl-2-butene followed by a subsequent isomerization which leaves the more electron-rich 1,1,2-trimethylallyl group as the η^3 ligand and the 3,3-dimethylallyl group as the η^1 -ligand in the solid state (eq 7). The mono-



hapticity of the dimethylallyl ligand is indicated by its orientation away from the metal center and the $\text{C}(11)\text{--C}(12)$ and $\text{C}(12)\text{--C}(13)$ bond lengths of 1.500(6) and 1.342(7) Å typical of a C–C single and double bond, respectively. Another clear indication of the loss of its previous η^3 coordination mode is the $\text{W}(1)\text{--C}(11)\text{--C}(12)$ bond angle of $113.3(3)^\circ$ which is reflective of principally sp^3 character at $\text{C}(11)$. Consistently, the most notable aspect of the ^1H NMR spectrum of **21** in C_6D_6 is the significant downfield shift of the signal due to the β -hydrogen of the η^1 -allyl fragment (δ 5.82) from its previous values (δ 3.54–4.43),

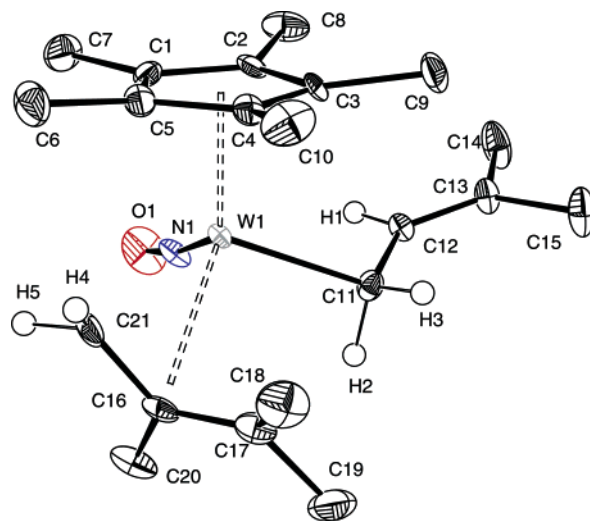
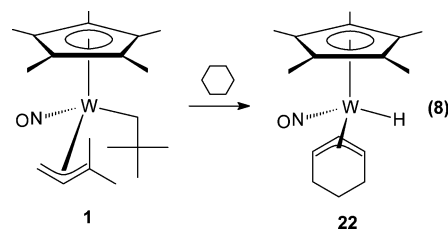


Figure 7. Solid-state molecular structure of $\text{Cp}^*\text{W}(\text{NO})(\eta^3\text{-Me}_2\text{CCMeCH}_2)(\eta^1\text{-CH}_2\text{CHCMe}_2)$ (**21**) with 50% probability thermal ellipsoids shown. Selected interatomic distances (Å) and angles (deg): $\text{W1--C11} = 2.236(5)$, $\text{C11--C12} = 1.500(6)$, $\text{C12--C13} = 1.342(7)$, $\text{W1--C21} = 2.219(5)$, $\text{W1--C16} = 2.403(5)$, $\text{W1--C17} = 2.696(5)$, $\text{C21--C16} = 1.438(7)$, $\text{C16--C17} = 1.375(7)$, $\text{N1--O1} = 1.221(5)$, $\text{C17--C16--C21} = 119.9(5)$, $\text{C11--C12--C13} = 130.3(5)$, $\text{W1--C11--C12} = 113.3(3)$, $\text{W1--N1--O1} = 170.9(4)$, $\text{C14--C13--C15} = 114.4(4)$, $\text{W1--C21--C16} = 79.0(3)$.

a feature indicative of the loss of metal-to-ligand electron density transfer that exists in the η^3 -allyl mode.

Multiple C–H Bond Activations Initiated by 1. (A) Activation of Cyclohexane. Reaction of **1** with cyclohexane leads to the formation of the cyclohexenyl-hydrido complex, $\text{Cp}^*\text{W}(\text{NO})(\eta^3\text{-C}_6\text{H}_9)(\text{H})$ (**22**) (eq 8), which has been characterized by conventional spectroscopic techniques.⁴⁴ This transformation constitutes a novel mode of multiple C–H activations of cyclohexane, a relatively inert solvent that has frequently been used to study the C–H activations of other hydrocarbons.^{45–47} In addition to complex **22**, GC-MS data suggest that a coupled organic product, a dimethylpropylcyclohexane, is also present in the final reaction mixture. This product could possibly result from coupling between a coordinated cyclohexenyl group and an alkyl fragment derived from the precursor dimethylallyl ligand.



For comparison, the well-studied bis(alkyl) complex, $\text{Cp}^*\text{W}(\text{NO})(\text{CH}_2\text{CMe}_3)_2$, reacts with cyclohexane in a completely different manner. Its thermolysis in the presence of an excess of trimethylphosphine in cyclohexane at 70°C for 40 h results

(38) Yasuoka, N.; Morita, M.; Kai, Y.; Kasai, N. *J. Organomet. Chem.* **1975**, *90*, 111.

(39) Lee, L.; Wu, I. Y.; Lin, Y. C.; Lee, G. H.; Wang, Y. *Organometallics* **1994**, *13*, 2521.

(40) Okamoto, K.; Kai, Y.; Yasuoka, N.; Kasai, N. *J. Organomet. Chem.* **1974**, *65*, 427.

(41) Yin, J.; Abboud, K. A.; Jones, W. M. *J. Am. Chem. Soc.* **1993**, *115*, 3810.

(42) The exceptionally strong π -donor ability of the related $\text{Cp}^*\text{W}(\text{NO})(\text{PPh}_3)_3$ fragment has been documented, see: Burke, D. J.; Debad, J. D.; Legzdins, P. *J. Am. Chem. Soc.* **1997**, *119*, 1139.

(43) Gibson, V. C.; Parkin, G.; Bercaw, J. E. *Organometallics* **1991**, *10*, 220.

(44) Preliminary single-crystal X-ray crystallographic analysis of **22** has confirmed the atomic connectivity shown in eq 8. However, the quality of the diffraction data collected precludes meaningful discussion of its metrical parameters.

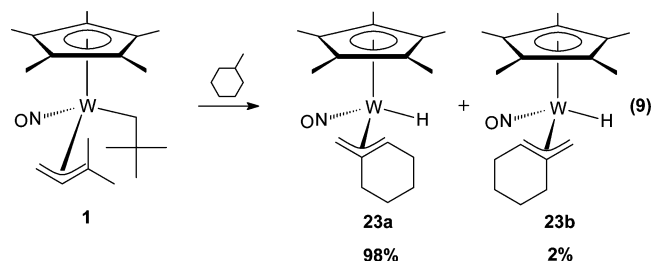
(45) McGhee, W. D.; Bergman, R. G. *J. Am. Chem. Soc.* **1988**, *110*, 4246.

(46) Cummins, C. C.; Baxter, S. M.; Wolczanski, P. T. *J. Am. Chem. Soc.* **1988**, *110*, 8731.

(47) Schaller, C. P.; Cummins, C. C.; Wolczanski, P. T. *J. Am. Chem. Soc.* **1996**, *118*, 591.

in the formation of two base-stabilized complexes, $\text{Cp}^*\text{W}(\text{NO})(=\text{CHCMe}_3)(\text{PMe}_3)$ and $\text{Cp}^*\text{W}(\text{NO})(\eta^2\text{-cyclohexene})(\text{PMe}_3)$.⁴⁸ However, in the absence of a suitable Lewis base, decomposition occurs. In contrast, the thermal reaction of **1** in cyclohexane in the presence of excess trimethylphosphine results in the exclusive formation of the PMe_3 -stabilized allene complex **20**.

(B) Activation of Methylcyclohexane. Two principal products are formed in the reaction between **1** and methylcyclohexane, the two isomeric species, $\text{Cp}^*\text{W}(\text{NO})(\eta^3\text{-C}_7\text{H}_{11})(\text{H})$ (**23a,b**) (eq 9).



Compounds **23a,b** are identical to the principal organometallic species isolated from the reactions of the intermediate tungsten neopentylidene and benzylidene species, $\text{Cp}^*\text{W}(\text{NO})(=\text{CHCMe}_3)$ and $\text{Cp}^*\text{W}(\text{NO})(=\text{CHC}_6\text{H}_5)$, with methylcyclohexane. The major product, **23a**, is formed in greater than 90% yield in all three cases, and it exhibits an exocyclic *endo*- η^3 -allyl linkage with the terminal CH_2 group being cis to the nitrosyl ligand. The apparent exclusive formation of exocyclic η^3 -allyl complexes as opposed to the endocyclic species suggests that the reactive intermediates preferentially activate the thermodynamically stronger primary C–H bonds, much like other metal-based alkane activation systems.⁴⁹

Conclusion

This work constitutes the first definitive demonstration of the C–H bond-activating ability of a transition-metal allene complex. Similar allene intermediates are believed to form during thermolyses of alkyl-allyl complexes of iridium at 120 °C, but these intermediates have not been isolated or characterized and they are only capable of effecting single C–H bond activations.⁴⁵ The studies presented here indicate the concurrent generation of a diene reactive species which is also evidently responsible for the C–H bond-activating chemistry initiated by **1**. However, cyclohexene is the only hydrocarbon substrate found to date that reacts with **1** under thermal conditions to form two different products resulting from the two reactive intermediates invoked. All other hydrocarbon solvents afford the same product regardless of which intermediate is involved in the activation of its C–H bonds. These studies have also elucidated the scope of single C–H bond activations via thermal reactions of **1** in the chosen hydrocarbon solvents. The thermodynamic preference for aromatic C–H activations over benzylic ones is evident in the product distributions resulting from the thermolyses of **1** with *p*- and *m*-xylene and toluene. Similar reactions conducted with *o*-xylene and mesitylene yield product ratios that suggest that steric factors play a role during benzylic and aromatic C–H activations initiated by **1**. Some of

the C–H activations effected by this system have been the subjects of theoretical studies.⁵⁰

There is no evidence for the formation of the bis(trimethylsilylmethyl), the benzyl-aryl, or the bis(mesityl) $\text{Cp}^*\text{W}(\text{NO})$ -containing complexes upon reaction of **1** in tetramethylsilane, toluene and xylenes, or mesitylene, respectively. This observation indicates that the dimethylallyl ligand in the products resulting from single C–H bond activation is not prone to elimination from the metal's coordination sphere to form reactive alkylidene and benzylidene species which have been demonstrated to have C–H-activating abilities.^{13,20} However, the formation of the allyl-hydrido complexes **22** and **23a,b** by thermolysis of **1** in cyclic alkanes must involve the ejection of the dimethylallyl moiety at some point, presumably via an initial $\eta^3 \rightarrow \eta^1$ isomerization of the type that has been shown to occur during the formation of the η^1 -dimethylallyl ligand in complex **21**. Furthermore, the reaction of **1** with methylcyclohexane gives an indication of the selectivity of the C–H-activating intermediate complexes for different sp^3 C–H bonds. The exclusive formation of the exocyclic allyl complexes **23a,b** suggests the preference of **A** and **B** to activate primary C–H bonds, a feature commonly observed for other metal-based alkane C–H-activating complexes.

Given the range of hydrocarbon solvents with which they have been shown to react to date, the C–H-activating chemistry of the reactive allene and diene intermediates appears to be quite extensive. It is also not unreasonable to expect that intramolecular hydrogen abstraction by other metal nitrosyl alkyl allyl complexes to eliminate alkanes and generate reactive intermediates will afford similarly diverse chemistry. Our studies designed to encompass both other hydrocarbon substrates and related C–H-activating intermediates are currently in progress.

Experimental Section

General Methods. All reactions and subsequent manipulations involving organometallic reagents were performed under anaerobic and anhydrous conditions either under high vacuum or an inert atmosphere of prepurified argon or dinitrogen. General procedures routinely employed in these laboratories have been described in detail elsewhere.^{20,51} All solvents were dried with appropriate drying agents under dinitrogen or argon atmospheres and were freshly distilled or vacuum transferred from the appropriate drying agent prior to use. Hydrocarbon solvents, their deuterated analogues, diethyl ether, and trimethylphosphine were dried over sodium or sodium/benzophenone ketyl. Tetrahydrofuran was distilled from molten potassium, and dichloromethane and chloroform were distilled from calcium hydride. All IR samples were prepared as KBr pellets, and their spectra were recorded on a BOMEM MB-100 FT-IR spectrometer unless otherwise noted. Elemental analyses were performed by Mr. P. Borda and Mr. M. Lakha in the Department of Chemistry at UBC and by Ms. Pauline Maloney of Canadian Microanalytical Service Ltd. in Delta B.C.

Unless otherwise specified, all reagents were purchased from commercial suppliers and were used as received. The $(\text{CH}_2\text{CMe}_3)_2\text{Mg}\cdot x(\text{dioxane})$ alkylating reagent and the requisite $\text{Cp}^*\text{W}(\text{NO})(\text{CH}_2\text{-CMe}_3)\text{Cl}$ complex were prepared according to published procedures.^{52,53} A modified version of the general synthetic method for dialkylmag-

(48) Tran, E.; Legzdins, P. *J. Am. Chem. Soc.* **1997**, *119*, 5071.

(49) Arndtsen, B. A.; Bergman, R. G.; Mobley, T. A.; Peterson, T. H. *Acc. Chem. Res.* **1995**, *28*, 154.

(50) Webster, C. E.; Hall, M. B. 224th ACS National Meeting, Boston, MA, August 2002; Abstract INOR-013.

(51) Legzdins, P.; Rettig, S. J.; Ross, K. J.; Batchelor, R. J.; Einstein, F. W. B. *Organometallics* **1995**, *14*, 5579.

(52) Dryden, N. H.; Legzdins, P.; Trotter, J.; Yee, V. C. *Organometallics* **1991**, *10*, 2857.

(53) Debad, J. D.; Legzdins, P.; Batchelor, R. J.; Einstein, F. W. B. *Organometallics* **1993**, *12*, 2094.

nesium reagents was employed for the preparation of the dimethylallylmagnesium reagent, and the procedure is described below.

Preparation of (1,1-Me₂C₃H₃)₂Mg·x(dioxane). 3,3-Dimethylallyl bromide (Fluka, 10 mL, 0.085 mol) was syringed into a 200-mL two-neck, round-bottom flask and was diluted with Et₂O (100 mL). In a glovebox, a 500-mL three-neck, round-bottom flask was charged with magnesium powder (4.2 g, 0.172 mol) and a magnetic stir bar. The 500-mL flask was transferred to a vacuum line, was charged with Et₂O (250 mL), and was fitted with a reflux condenser. Activation of the magnesium powder was accomplished via addition of sufficient dibromoethane (~1–2 mL) using a syringe. The suspension was allowed to reflux until all of the added dibromoethane had reacted. The suspension was then cooled in an ice bath to 0 °C, whereupon the ethereal bromide solution was added dropwise via a cannula over a 3-h period. During this time, the contents of the flask were stirred rapidly, and the solution remained clear. Upon completion of the dropwise addition, the mixture was slowly warmed to room temperature. The transformation of the Grignard reagent into the bis(allyl)magnesium reagent was conducted in the usual manner.⁵² (1,1-Me₂C₃H₃)₂Mg·x(dioxane) was isolated as a snow-white powder (2.7 g, 50%), and titration with 0.1 M HCl afforded a titer of 127 g/mol.

Cp*W(NO)(CH₂CMe₃)(η³-1,1-Me₂C₃H₃) (1). In a glovebox, a 100-mL Schlenk tube was charged with a magnetic stir bar and Cp*W(NO)(CH₂CMe₃)Cl (483 mg, 1.15 mmol).⁵⁴ A 400-mL Schlenk tube was then charged with a magnetic stir bar and the dimethylallylmagnesium reagent (147 mg, 1.16 mmol). On a vacuum line, Et₂O (200 mL) from a bomb was cannulated into the Schlenk tube containing the magnesium reagent with vigorous stirring to ensure its dissolution. The resulting colorless solution was then frozen by cooling to –196 °C using a liquid N₂ bath. Et₂O (50 mL) was added in a similar fashion to the Schlenk tube containing the solid Cp*W(NO)(CH₂CMe₃)Cl to obtain a purple solution which was then cooled to –60 °C with a dry ice/acetone bath. The purple solution was then cannulated dropwise into the 400-mL Schlenk tube (maintained at –196 °C) at a slow enough rate that allowed the added solution to freeze upon contact with the solidified ethereal solution of the magnesium reagent. Sufficient Et₂O was added to the 100-mL Schlenk tube and subsequently cannulated into the reaction flask to ensure complete transfer of Cp*W(NO)(CH₂CMe₃)Cl. The liquid N₂ bath was replaced with a liquid N₂/acetone bath at –60 °C to enable the ethereal contents to melt slowly. After being stirred for 5 min, the purple solution changed to a straw-yellow color which then became a turbid orange after a further 10 min. The solution was stirred at –60 °C for a total of 45 min, whereupon the contents were warmed to room temperature to ensure completion of the reaction. The volume of the mixture was reduced under vacuum to ~100 mL, and the turbid orange solution was filtered through an alumina(I) column (2 × 3 cm) which was also rinsed with fresh Et₂O (2 × 10 mL) to obtain a clear bright orange filtrate. The volatiles were then removed from the filtrate in vacuo to obtain an orange crystalline powder which was dried at room temperature under high vacuum for 1 h. Analysis of this solid by ¹H NMR spectroscopy revealed that complex **1** was the sole organometallic product. Analytically pure **1** was obtained as orange microcrystals (296 mg, 57%) via crystallization from a THF/hexanes mixture (5 mL/20 mL) at –25 °C.

1: IR (cm^{–1}) 1546 (s, ν_{NO}). MS (LREI, *m/z*, probe temperature 150 °C) 489 [P⁺, ¹⁸⁴W]. ¹H NMR (300 MHz, C₆D₆) δ 0.67 (s, 3H, allyl Me), 1.02 (obs, 1H, Npt CH₂), 1.02 (s, 3H, allyl Me), 1.42 (s, 9H, Npt CMe₃), 1.42 (obs, 1H, allyl CH₂), 1.53 (s, 15H, C₅Me₅), 2.69 (m, 1H, allyl CH₂), 4.45 (m, 1H, allyl CH). ¹H NMR (400 MHz, CD₂Cl₂) δ 0.88 (d, ²J_{HH} = 14.2, 1H, Npt CH₂), 0.99 (s, 3H, allyl Me), 1.02 (d, ²J_{HH} = 14.2, 1H, Npt CH₂), 1.06 (s, 9H, Npt CMe₃), 1.24 (s, 3H, allyl Me), 1.61 (m, 1H, allyl CH₂), 1.82 (s, 15H, C₅Me₅), 2.55 (m, 1H, allyl CH₂), 4.40 (m, 1H, allyl CH). ¹³C{¹H} NMR (75 MHz, CD₂Cl₂) δ

10.2 (C₅Me₅), 19.5, 30.7 (allyl Me), 34.3 (Npt CMe₃), 37.6 (allyl CH₂), 39.9 (Npt CMe₃), 40.7 (Npt CH₂), 101.7 (allyl CH), 107.5 (C₅Me₅), 147.8 (allyl C). Sel NOE (400 MHz, C₆D₆) δ irradi. at 4.45, NOE at 1.02, irradi. at 0.67, NOE at 1.02, 1.42, 1.52, and 2.55. Anal. Calcd for C₂₀H₃₅NO: C, 49.09; H, 7.21; N, 2.86. Found: C, 49.16; H, 7.03; N, 2.87.

Representative Procedure for Effecting Preparative Thermolyses of 1 in Hydrocarbon Solvents. Unless noted otherwise, the following general procedure was used to prepare new compounds via thermolysis of **1**. A 30-mL bomb was charged with the specified amount of **1**, a magnetic stir bar, and sufficient solvent to obtain an approximately 10% (w/w) orange solution. The solvent was either pipetted directly into the reaction vessel from a storage bomb inside a glovebox or vacuum transferred onto the orange microcrystals on a vacuum line. The sealed bomb was then heated at 50 °C for a period of 6 h in a VWR Scientific Products Circulating Bath 1160A. During this time, the deep orange color of the reaction mixture either remained unchanged or lightened to an orange-yellow. Alternatively, it darkened to a brown color, whereupon further steps were necessary to extract and isolate the analytically pure organometallic products. The reaction bomb was removed from the bath, and the reaction was quenched by placing the bomb under a flow of cold water or dipping it into a cold bath. The volatiles were then removed in vacuo, and the resulting residue was dried under high vacuum for a suitable period of time. It was then dissolved in C₆D₆, and the ¹H NMR spectrum of this mixture was recorded to determine the number of principal organometallic products present and the ratios in which they were formed. Average product ratios were determined via multiple integrations of like signals in this ¹H NMR spectrum. The NMR solvent was then removed, and the residue was redissolved in the specified solvent or solvent mixtures for recrystallization of the products. The solutions were then concentrated to the point of incipient crystallization and cooled for a suitable amount of time at –30 °C to induce the deposition of the organometallic products as crystals. The reported yields are not optimized.

Cp*W(NO)(CH₂SiMe₃)(η³-1,1-Me₂C₃H₃) (2). Complex **2** was prepared via thermolysis of **1** (75 mg, 0.15 mmol) in tetramethylsilane. The reaction mixture was then cooled overnight in a freezer (–30 °C) to obtain orange needles of **2** (47 mg, 61%).

2: IR (cm^{–1}) 1549 (s, ν_{NO}). MS (LREI, *m/z*, probe temperature 80 °C) 505 [P⁺, ¹⁸⁴W]. ¹H NMR (400 MHz, C₆D₆) δ –0.78 (d, ²J_{HH} = 14.09, 1H, SiCH₂), –0.59 (d, ²J_{HH} = 14.09, 1H, SiCH₂), 0.45 (s, 9H, SiMe₃), 0.61 (s, 3H, allyl Me), 1.12 (s, 3H, allyl Me), 1.18 (m, 1H, allyl CH₂), 1.51 (s, 15H, C₅Me₅), 2.55 (m, 1H, allyl CH₂), 4.43 (m, 1H, allyl CH). ¹³C{¹H} NMR (125 MHz, C₆D₆) δ 2.01 (SiCH₂), 4.34 (SiMe₃), 10.2 (C₅Me₅), 19.6, 28.9 (allyl Me), 39.3 (allyl CH₂), 101.9 (allyl CH), 106.9 (C₅Me₅). Sel NOE (400 MHz, C₆D₆) δ irradi. at 0.61, NOE at –0.78, 0.45, 1.12, 1.18, 1.51, and 2.55. Anal. Calcd for C₁₉H₃₅NOSiW: C, 45.15; H, 6.98; N, 2.77. Found: C, 45.37; H, 6.92; N, 2.90.

Cp*W(NO)(CH₂C₆H₃-3,5-Me₂)(η³-1,1-Me₂C₃H₃) (3). Complex **3** was prepared by the thermolysis of **1** (79 mg, 0.16 mmol) in mesitylene. The volume was reduced to 2 mL, and hexanes (10 mL) were added via a syringe. Cooling of the mixture resulted in the precipitation of **3** as orange microcrystals (57 mg, 66%).

3: IR (cm^{–1}) 1533 (s, ν_{NO}). MS (LREI, *m/z*, probe temperature 120 °C) 537 [P⁺, ¹⁸⁴W]. ¹H NMR (400 MHz, C₆D₆) δ 1.08 (s, 3H, allyl Me), 1.17 (s, 3H, allyl Me), 1.46 (s, 15H, C₅Me₅), 1.52 (obs, 1H, allyl CH₂), 1.79 (d, ²J_{HH} = 9.46, 1H, Mes CH₂), 2.38 (s, 6H, Mes Me₂), 2.45 (m, 1H, allyl CH₂), 2.80 (d, ²J_{HH} = 9.46, 1H, Mes CH₂), 3.58 (s, 1H, allyl CH), 6.72 (s, 1H, Mes H_{para}), 7.38 (s, 2H, Mes H_{ortho}). ¹³C{¹H} NMR (125 MHz, C₆D₆) δ 9.88 (C₅Me₅), 20.63 (allyl Me), 22.03 (Mes Me₂), 27.65 (allyl Me), 28.23 (allyl CH₂), 39.69 (Mes CH₂), 98.86 (allyl CH), 106.49 (C₅Me₅), 125.24 (Mes *p*-CH), 128.70 (Mes *o*-CH), 152.4 (allyl C), 136.5, 169.2 (C_{aryl}). Sel NOE (400 MHz, C₆D₆) δ irradi. at 3.58, NOE at 1.08, 1.52, 2.45, irradi. at 1.08, NOE at 1.17, 1.46,

(54) Our previous communication of the chemistry exhibited by **1** (see ref 4) incorrectly designated the dimethylallyl ligand as 3,3-Me₂C₃H₃.

1.79, 2.80, 3.58, and 7.38. Anal. Calcd for $C_{24}H_{35}NO$: C, 53.64; H, 6.56; N, 2.61. Found: C, 53.80; H, 6.61; N, 2.75.

Cp*W(NO)(C₆H₅)(η^3 -1,1-Me₂C₃H₃) (4). Complex **4** was formed during the thermolysis of **1** (48 mg, 0.10 mmol) in benzene. Complex **4** was isolated as yellow microcrystals by recrystallization of the residue from 4:1 Et₂O/hexanes (34 mg, 70%).

4: IR (cm⁻¹) 1562 (s, ν_{NO}). MS (LREI, m/z , probe temperature 150 °C) 495 [P⁺, ¹⁸⁴W]. ¹H NMR (300 MHz, C₆D₆) δ 0.82 (s, 3H, allyl Me), 1.51 (s, 15H, C₅Me₅), 1.62 (br s, 3H, allyl Me), 1.74 (br m, 1H, allyl CH₂), 2.49 (br m, 1H, allyl CH₂), 3.54 (br m, 1H, allyl CH), 6.64 (br d, 1H, Ph H_{ortho}), 7.08 (t, ³J_{HH} = 7.1, 1H, Ph H_{para}), 7.30 (m, 2H, Ph H_{meta}), 8.39 (d, ³J_{HH} = 6.7, 1H, Ph H_{ortho}). ¹H NMR (400 MHz, CDCl₃) δ 0.87 (s, 3H, allyl Me), 1.51 (br s, 3H, allyl Me), 1.76 (s, 15H, C₅Me₅), 1.90 (br m, 1H, allyl CH₂), 2.42 (br m, 1H, allyl CH₂), 3.73 (br m, 1H, allyl CH), 6.68 (br d, 1H, Ph H_{ortho}), 6.93 (t, ³J_{HH} = 7.1, 1H, Ph H_{para}), 7.12 (q, ³J_{HH} = 7.0, 2H, Ph H_{meta}), 7.86 (d, ³J_{HH} = 6.4, 1H, Ph H_{ortho}). ¹³C{¹H} NMR (75 MHz, CDCl₃) δ 10.4 (C₅Me₅), 21.8, 29.4 (allyl Me), 37.6 (allyl CH₂), 95.3 (allyl CH), 107.6 (C₅-Me₅), 123.4 (Ph C_{para}), 126.8, 127.9 (Ph C_{meta}), 139.6, 141.9 (Ph C_{ortho}), 148.5 (allyl C), 168.8 (Ph C_{ipso}). Sel NOE (400 MHz, C₆D₆) δ irradi. at 3.54, NOE at 0.82, 1.51, and 1.74, irradi. at 0.82, NOE at 1.51, 1.63, 3.54, 6.64, 8.39. Anal. Calcd for C₂₁H₂₉NO: C, 50.92; H, 5.90; N, 2.83. Found: C, 50.61; H, 5.95; N, 2.92.

Cp*W(NO)(C₆D₅)(η^3 -1,1-Me₂-allyl-d₁) (4a–c-d₆). Complexes **4a–c-d₆** were prepared by the thermolysis of **1** (10 mg, 0.02 mmol) in benzene-d₆. Yellow crystals of complexes **4a–c-d₆** were obtained via crystallization of the residue from 4:1 Et₂O/hexanes.

4a–c-d₆: MS (LREI, m/z , probe temperature 120 °C) 501 [P⁺, ¹⁸⁴W]. ¹H NMR (400 MHz, C₆D₆) δ 0.82 (s, 3H, allyl Me), 1.51 (s, 15H, C₅Me₅), 1.62 (br s, 3H allyl Me), 1.73 (br m, 1H, allyl CH₂), 2.48 (br m, 1H, allyl CH₂), 3.52 (br m, 1H, allyl CH). ²H{¹H} NMR (61 MHz, C₆H₆) δ 0.78 (allyl Me-d₁), 1.61 (allyl Me-d₁), 3.52 (allyl CD), 6.60–8.4 (Ph D).

Reaction Products of Thermolyses of 1 in Toluene and *o,m,p*-Xylenes. Thermolyses of **1** in toluene and xylene solvents afforded final reaction mixtures with multiple organometallic products due to the activation of different C–H bonds present in the hydrocarbons. For the various reaction mixtures, the residues remaining after the reaction solvent had been removed were triturated with pentane (3 × 10 mL) to alleviate the oily appearance. Solid product was isolated via crystallization from hexanes. It was then possible to separate the benzylic C–H-activated product from the aryl C–H-activated species either via preparative thin-layer chromatography on an alumina(I) plate (20 × 20 × 0.15 cm) or via column chromatography through an alumina(I) column (0.5 × 3 cm). The former separation technique was utilized once for the products from reaction of **1** in *p*-xylene (vide infra). The latter technique was employed for the remainder of the product separations. The products isolated via crystallization were dissolved in a 1:5 Et₂O/hexanes solvent mixture, and the resulting solution was eluted through the column described above which was pretreated with the eluting solvent. A yellow eluate resulted which upon concentration and cooling to –30 °C overnight deposited solely the aryl C–H-activated products. Eluting the column with 1:4 Et₂O/hexanes gave a solution consisting of small amounts of both aryl and benzylic C–H-activated species. Stripping the alumina column with Et₂O yielded an orange solution which upon addition of hexanes and then subsequent concentration and cooling to –30 °C overnight yielded solely the benzylic C–H-activated product.

Cp*W(NO)(CH₂C₆H₄-4-Me)(η^3 -1,1-Me₂C₃H₃) (5) and Cp*W(NO)(C₆H₃-2,5-Me₂)(η^3 -1,1-Me₂C₃H₃) (6). Complexes **5** and **6** were formed via the thermolysis of **1** (292 mg, 0.60 mmol) in *p*-xylene. The resulting residue following removal of solvent was an orange/yellow oil. The solid products obtained after workup (vide supra) were dissolved in a minimal amount of THF, and the resulting solution was applied to a preparative-TLC plate using a syringe with a 26-gauge needle to obtain a 10-mm wide orange/yellow band. The plate was left

to sit for 30 min to allow evaporation of the THF solvent, and it was then loaded into a development chamber charged with Et₂O (200 mL) and sealed to minimize solvent loss and ensure maximum vapor saturation. After 70 min of development, the plate was removed from the chamber and allowed to dry. No clear separation was evident, but a definite region where the band was lighter in color was visible. The alumina above this region was scraped off and stripped of any organometallic product with THF and subsequently filtered thru a Celite plug to obtain a yellow solution. Removal of solvent from this solution and recrystallization of the residue from 1:4 Et₂O/hexanes afforded yellow needles of complex **6** (53 mg, 17%). The alumina below the lighter region was treated in a similar fashion to obtain orange needles of complex **5** (24 mg, 8%).

5: IR (cm⁻¹) 1553 (s, ν_{NO}). MS (LREI, m/z , probe temperature 120 °C) 523 [P⁺, ¹⁸⁴W]. ¹H NMR (400 MHz, C₆D₆) δ 1.07 (s, 3H, allyl Me), 1.15 (s, 3H, allyl Me), 1.46 (s, 15H, C₅Me₅), 1.46 (obs, 1H, allyl CH₂), 1.80 (m, 1H, ²J_{HH} = 11.6, Bzl CH₂), 2.26 (s, 3H, Pxylyl Me), 2.43 (m, 1H, allyl CH₂), 2.77 (m, 1H, ²J_{HH} = 11.6, Bzl CH₂), 3.56 (m, 1H allyl CH), 7.13 (obs, 2H, Pxylyl *m*-CH), 7.62 (d, 2H, ³J_{HH} = 7.6, Pxylyl *o*-CH). ¹³C{¹H} NMR (100 MHz, C₆D₆) δ 9.7 (C₅Me₅), 20.5 (allyl Me), 21.0 (Pxylyl Me), 27.4 (allyl Me), 35.2 (Bzl CH₂), 39.6 (allyl CH₂), 98.3 (allyl CH), 106.3 (C₅Me₅), 124.8 (Pxylyl *p*-CH), 128.0 (obs Pxylyl *o*-CH), 130.4 (Pxylyl *m*-CH), 149.8 (allyl C). Anal. Calcd for C₂₃H₃₃NO: C, 52.78; H, 6.36; N, 2.68. Found: C, 52.66; H, 6.26; N, 2.75.

6: IR (cm⁻¹) 1567 (s, ν_{NO}). MS (LREI, m/z , probe temperature 120 °C) 523 [P⁺, ¹⁸⁴W]. ¹H NMR (500 MHz, C₆D₆) δ 0.80 (s, 3H, allyl Me), 1.54 (s, 15H, C₅Me₅), 1.74 (s, 3H, allyl Me), 1.79 (m, 1H, allyl CH₂), 2.18 (s, 3H, Xyl Me), 2.50 (m, 1H, allyl CH₂), 2.80 (s, 3H, Xyl Me), 3.70 (m, 1H, allyl CH), 6.12 (s, 1H, Xyl *o*-CH), 6.77 (d, 1H, ³J_{HH} = 7.4, Xyl CH), 7.25 (d, 1H, ³J_{HH} = 7.4, Xyl CH). ¹³C{¹H} NMR (125 MHz, C₆D₆) δ 10.2 (C₅Me₅), 21.0 (Xyl Me), 22.6 (allyl Me), 27.6 (Xyl Me), 28.6 (allyl Me), 39.6 (allyl CH₂), 96.1 (allyl CH), 107.3 (C₅Me₅), 124.8 (Xyl CH), 130.4 (Xyl CH), 140.4 (Xyl *o*-CH), 148.0 (allyl C), 170.3 (Xyl C_{ipso}). Anal. Calcd for C₂₃H₃₃NO: C, 52.78; H, 6.36; N, 2.68. Found: C, 52.67; H, 6.26; N, 2.66.

Cp*W(NO)(CH₂C₆H₄-3-Me)(η^3 -1,1-Me₂C₃H₃) (7), Cp*W(NO)-(C₆H₃-2,4-Me₂)(η^3 -1,1-Me₂C₃H₃) (8), and Cp*W(NO)(C₆H₃-3,5-Me₂)(η^3 -1,1-Me₂C₃H₃) (9). Complexes **7–9** were prepared via the thermolysis of **1** (100 mg, 0.20 mmol) in *m*-xylene. The resulting residue following removal of solvent was an orange/yellow oil. Subsequent workup and separation of products afforded complex **7** as orange blocks (15 mg, 14%) and a mixture of complexes **8** and **9** as orange/yellow microcrystals (40 mg, 37%).

7: IR (cm⁻¹) 1560 (s, ν_{NO}). MS (LREI, m/z , probe temperature 120 °C) 523 [P⁺, ¹⁸⁴W]. ¹H NMR (400 MHz, C₆D₆) δ 1.06 (s, 3H, allyl Me), 1.11 (s, 3H, allyl Me), 1.45 (s, 15H, C₅Me₅), 1.53 (m, 1H, allyl CH₂), 1.79 (d, 1H, ²J_{HH} = 11.4, Mxyl CH₂), 2.38 (s, 3H, Mxyl Me), 2.46 (m, 1H, allyl CH₂), 2.81 (d, 1H, ²J_{HH} = 11.4, Mxyl CH₂), 3.54 (m, 1H, allyl CH), 6.89 (d, 1H, ³J_{HH} = 7.3, Mxyl CH), 7.27 (t, 1H, ³J_{HH} = 7.5, Mxyl CH), 7.54 (d, 1H, ³J_{HH} = 7.8, Mxyl CH), 7.58 (s, 1H, Mxyl *o*-CH). ¹³C{¹H} NMR (100 MHz, C₆D₆) δ 9.7 (C₅Me₅), 22.0 (Mxyl Me), 27.5 (allyl Me), 27.8 (Mxyl CH₂), 39.6 (allyl CH₂), 98.2 (allyl CH), 106.3 (C₅Me₅), 124.0 (Mxyl CH), 128.0 (obs Mxyl CH), 128.0 (obs Mxyl CH), 131.4 (Mxyl CH), 136.5 (Mxyl C), 153.0 (allyl C). Anal. Calcd for C₂₃H₃₃NO: C, 52.78; H, 6.36; N, 2.68. Found: C, 52.76; H, 6.20; N, 2.71.

8,9: IR (cm⁻¹) 1552 (s, ν_{NO}). MS (LREI, m/z , probe temperature 120 °C) 523 [P⁺, ¹⁸⁴W]. Anal. Calcd for C₂₃H₃₃NO: C, 52.78; H, 6.36; N, 2.68. Found: C, 52.54; H, 6.43; N, 2.83.

8: ¹H NMR (400 MHz, C₆D₆) δ 0.81 (s, 3H, allyl Me), 1.54 (s, 15H, C₅Me₅), 1.74 (s, 3H, allyl Me), 1.78 (m, 1H, allyl CH₂), 2.28 (s, 3H, Xyl Me), 2.49 (m, 1H, allyl CH₂), 2.82 (s, 3H, Xyl Me), 3.71 (m, 1H, allyl CH), 6.22 (d, 1H, ²J_{HH} = 7.4, Xyl CH), 6.82 (d, 1H, ²J_{HH} = 7.4, Xyl CH), 7.15 (obs, 1H, Xyl CH). ¹³C{¹H} NMR (100 MHz, C₆D₆) δ 10.3 (C₅Me₅), 21.2 (Xyl Me), 23.0 (allyl Me), 28.4 (Xyl Me), 28.7

(allyl Me), 39.7 (Xyl Me), 96.0 (allyl CH), 107.0 (C_5Me_5), 124.7 (Xyl CH), 131.7 (Xyl CH), 139.3 (Xyl CH).

9: 1H NMR (400 MHz, C_6D_6) δ 0.86 (s, 3H, allyl Me), 1.55 (s, 15H, C_5Me_5), 1.65 (bs, 3H, allyl Me), 1.77 (m, 1H, allyl CH_2), 2.28 (s, 3H, Xyl Me), 2.34 (s, 3H, Xyl Me), 2.50 (m, 1H, allyl CH_2), 3.56 (bm, 1H, allyl CH), 6.30 (bs, 1H, Xyl CH), 6.71 (s, 1H, Xyl CH), 8.04 (s, 1H, Xyl CH). $^{13}C\{^1H\}$ NMR (100 MHz, C_6D_6) δ 10.3 (C_5Me_5), 21.4 (Xyl Me), 21.6 (Xyl Me), 21.9 (allyl Me), 29.3 (allyl Me), 37.4 (allyl CH_2), 95.6 (allyl CH), 107.3 (C_5Me_5), 125.6 (Xyl CH), 138.3 (Xyl CH), 140.0 (Xyl CH).

$Cp^*W(NO)(CH_2C_6H_4-2-Me)(\eta^3-1,1-Me_2C_3H_3)$ (10), $Cp^*W(NO)(C_6H_3-2,3-Me_2)(\eta^3-1,1-Me_2C_3H_3)$ (11), and $Cp^*W(NO)(C_6H_3-3,4-Me_2)(\eta^3-1,1-Me_2C_3H_3)$ (12). Complexes **10–12** were formed by the thermolysis of **1** (205 mg, 0.42 mmol) in *o*-xylene. The resulting residue following removal of solvent was an orange/yellow oil. Subsequent workup and separation of products afforded complex **10** as orange microcrystals (21 mg, 10%) and a mixture of complexes **11** and **12** as orange/yellow microcrystals (56 mg, 26%).

10: IR (cm^{-1}) 1552 (s, ν_{NO}). MS (LREI, m/z , probe temperature 150 $^{\circ}C$) 523 [P^+ , ^{184}W]. 1H NMR (500 MHz, C_6D_6) δ 0.81 (m, 1H, allyl CH_2), 1.20 (s, 3H, allyl Me), 1.27 (s, 3H, allyl Me), 1.49 (s, 15H, C_5Me_5), 2.04 (m, 1H, allyl CH_2), 2.19 (d, 1H, $^3J_{HH} = 10.7$, Bzl CH_2), 2.36 (d, 1H, $^2J_{HH} = 10.7$, Bzl CH_2), 2.45 (s, 3H, Oxyl Me), 3.98 (m, 1H, allyl CH), 7.05 (m, 1H, Oxyl CH), 7.10 (obs 1H, Oxyl CH), 7.10 (obs, 1H, Oxyl CH), 7.23 (d, 1H, $^3J_{HH} = 7.0$, Oxyl CH). $^{13}C\{^1H\}$ NMR (125 MHz, C_6D_6) δ 9.7 (C_5Me_5), 20.3 (allyl Me), 21.5 (Oxyl Me), 26.9 (allyl Me), 26.9 (Bzl CH_2), 103.2 (allyl CH), 106.5 (C_5Me_5), 125.1 (Oxyl CH), 125.8 (Oxyl CH), 129.0 (Oxyl CH), 130.1 (Oxyl CH). Anal. Calcd for $C_{23}H_{33}NOW$: C, 52.78; H, 6.36; N, 2.68. Found: C, 53.02; H, 6.36; N, 2.92.

11,12: IR (cm^{-1}) 1552 (s, ν_{NO}). MS (LREI, m/z , probe temperature 150 $^{\circ}C$) 523 [P^+ , ^{184}W]. Anal. Calcd for $C_{23}H_{33}NOW$: C, 52.78; H, 6.36; N, 2.68. Found: C, 52.93; H, 6.37; N, 2.61.

11: 1H NMR (400 MHz, C_6D_6) δ 0.85 (s, 3H, allyl Me), 1.55 (s, 15H, C_5Me_5), 1.59 (s, 3H, allyl Me), 1.76 (obs, 1H, allyl CH_2), 2.21 (br s, 6H, 2 Xyl Me), 2.50 (m, 1H, allyl CH_2), 3.56 (br m, 1H, allyl CH), 6.45 (br s, 2H, 2 Xyl CH), 7.07 (d, 1H, $^3J_{HH} = 7.4$, Xyl CH). $^{13}C\{^1H\}$ NMR (100 MHz, C_6D_6) δ 10.3 (C_5Me_5), 19.6 (Xyl Me), 19.8 (Xyl Me), 24.7 (allyl Me), 28.4 (allyl Me), 37.4 (allyl CH_2), 95.9 (allyl CH), 106.9 (C_5Me_5), 128.8 (Xyl CH), 137.8 (Xyl CH), 141.7 (Xyl CH).

12: 1H NMR (400 MHz, C_6D_6) δ 0.88 (s, 3H, allyl Me), 1.55 (s, 15H, C_5Me_5), 1.65 (br s, 3H, allyl Me), 1.76 (obs, 1H, allyl CH_2), 2.18 (s, 3H, Xyl Me), 2.27 (s, 3H, Xyl Me), 2.50 (m, 1H, allyl CH_2), 3.56 (br s, 1H, allyl CH), 7.13 (obs, 1H, Xyl CH), 8.17 (obs, 1H, Xyl CH), 8.19 (s, 1H, Xyl CH). $^{13}C\{^1H\}$ NMR (100 MHz, C_6D_6) δ 10.3 (C_5Me_5), 19.5 (Xyl Me), 19.8 (Xyl Me), 21.8 (allyl Me), 29.4 (allyl Me), 37.3 (allyl CH_2), 95.8 (allyl CH), 106.9 (C_5Me_5), 130.2 (Xyl CH), 140.2 (Xyl CH), 143.7 (Xyl CH).

$Cp^*W(NO)(CH_2C_6H_5)(\eta^3-1,1-Me_2C_3H_3)$ (13), $Cp^*W(NO)(C_6H_4-2-Me)(\eta^3-1,1-Me_2C_3H_3)$ (14), $Cp^*W(NO)(C_6H_4-3-Me)(\eta^3-1,1-Me_2C_3H_3)$ (15), and $Cp^*W(NO)(C_6H_4-4-Me)(\eta^3-1,1-Me_2C_3H_3)$ (16). Complexes **13–16** were prepared via the thermolysis of **1** (200 mg, 0.41 mmol) in toluene. After the 6-h reaction period, the resulting solution was a dark orange/brown color which yielded a brown oil upon solvent removal under vacuum. Subsequent workup and separation of products afforded complex **13** and a mixture of complexes **14–16** as orange/yellow blocks (156 mg, 75%).

Complex **13** was prepared by a method similar to the procedure published for $Cp^*W(NO)(CH_2C_6H_5)(CH_2CMe_3)$.²⁰ In the glovebox, a 100-mL Schlenk tube was charged with a magnetic stir bar and (1,1- $Me_2C_3H_3$)₂Mg·x(dioxane) (103 mg, 0.53 mmol). A 200-mL Schlenk tube was then charged with a stir bar and $Cp^*W(NO)(CH_2C_6H_5)Cl$ (250 mg, 0.53 mmol). On a vacuum line, THF (80 mL) was vacuum transferred into the Schlenk tube containing the organometallic halide and into the Schlenk tube with the magnesium reagent (10 mL). The two resulting solutions were then mixed at $-78\ ^{\circ}C$ over a period of 5

min via a cannula, whereupon the initial deep-red color of the solution changed to orange/yellow after being stirred at $-78\ ^{\circ}C$ for 10 min. The final mixture was then warmed to $0\ ^{\circ}C$, and the reaction was allowed to proceed for 1 h. The solvent was then removed at $0\ ^{\circ}C$ over a period of 30 min. The residue was extracted with CH_2Cl_2 (3×10 mL), and the combined extracts were filtered through an alumina-(I) plug (2×3 cm) supported on a frit to obtain an orange filtrate. The CH_2Cl_2 was removed from the filtrate under vacuum, and the residue was recrystallized from a 2:1 Et_2O /hexanes mix at $-30\ ^{\circ}C$ to obtain complex **13** as yellow and orange blocks (138 mg, 52%).

13: IR (cm^{-1}) 1552 (s, ν_{NO}). MS (LREI, m/z , probe temperature 120 $^{\circ}C$) 509 [P^+ , ^{184}W]. 1H NMR (500 MHz, C_6D_6) δ 1.04 (s, 3H, allyl Me), 1.14 (s, 3H, allyl Me), 1.43 (s, 15H, C_5Me_5), 1.55 (br s, 1H, allyl CH_2), 1.78 (d, 1H, $^2J_{HH} = 11.5$, Bzl CH_2), 2.46 (m, 1H, allyl CH_2), 2.81 (d, 1H, $^2J_{HH} = 11.5$, Bzl CH_2), 3.52 (m, 1H, allyl CH), 7.03 (t, 1H, $^3J_{HH} = 7.4$, aryl *p*-CH), 7.32 (t, 2H, $^3J_{HH} = 7.4$, aryl *m*-CH), 7.71 (d, 2H, $^3J_{HH} = 7.4$, aryl *o*-CH). $^{13}C\{^1H\}$ NMR (125 MHz, C_6D_6) δ 9.7 (C_5Me_5), 20.5 (allyl Me), 27.5 (allyl Me), 27.8 (Bzl CH_2), 39.8 (allyl CH_2), 97.9 (allyl CH), 106.4 (C_5Me_5), 123.1 (aryl *p*-CH), 127.7 (aryl *m*-CH), 130.4 (aryl *o*-CH), 153.4 (allyl C). Anal. Calcd for $C_{22}H_{31}NOW$: C, 51.88; H, 6.13; N, 2.75. Found: C, 51.95; H, 6.25; N, 2.86.

14–16: IR (cm^{-1}) 1561 (s, ν_{NO}). MS (LREI, m/z , probe temperature 150 $^{\circ}C$) 509 [P^+ , ^{184}W]. Anal. Calcd for $C_{22}H_{31}NOW$: C, 51.88; H, 6.13; N, 2.75. Found: C, 51.84; H, 6.49; N, 2.85.

14: 1H NMR (400 MHz, C_6D_6) δ 2.26 (s, 3H, Tol Me), 3.55 (br m, 1H, allyl CH), 6.47 (br s, 1H, Tol CH), 6.88 (d, 1H, $^3J_{HH} = 7.1$, Tol CH), 7.25 (t, 1H, $^3J_{HH} = 7.1$, Tol CH), 8.21 (d, 1H, $^3J_{HH} = 7.1$, Tol CH). $^{13}C\{^1H\}$ NMR (100 MHz, C_6D_6) δ 10.2 (C_5Me_5), 21.7 (Tol Me), 95.8 (allyl CH), 106.9 (C_5Me_5), 124.8 (Tol CH), 128.0 (obs, Tol CH), 139.5 (Tol CH), 141.2 (Tol CH).

15: 1H NMR (400 MHz, C_6D_6) δ 2.35 (s, 3H, Tol Me), 3.55 (br m, 1H, allyl CH), 6.47 (br s, 1H, Tol CH), 6.94 (d, 1H, $^3J_{HH} = 6.6$, Tol CH), 7.16 (obs, 1H, Tol CH), 8.24 (s, 1H, Tol CH). $^{13}C\{^1H\}$ NMR (100 MHz, C_6D_6) δ 10.2 (C_5Me_5), 21.9 (Tol Me), 95.8 (allyl CH), 106.9 (C_5Me_5), 123.5 (Tol CH), 126.9 (Tol CH), 137.2 (Tol CH), 143.1 (Tol CH).

16: 1H NMR (400 MHz, C_6D_6) δ 2.28 (s, 3H, Tol Me), 3.55 (br m, 1H, allyl CH), 6.58 (br s, 1H, Tol CH), 7.08 (d, 1H, $^3J_{HH} = 6.6$, Tol CH), 7.16 (obs, 1H, Tol CH), 8.31 (d, 1H, $^3J_{HH} = 7.1$, Tol CH). $^{13}C\{^1H\}$ NMR (100 MHz, C_6D_6) δ 10.2 (C_5Me_5), 21.5 (Tol Me), 95.8 (allyl CH), 106.9 (C_5Me_5), 128.0 (obs Tol CH), 129.6 (Tol CH), 140.1 (Tol CH), 142.4 (Tol CH).

$Cp^*W(NO)(\eta^4-trans-H_2C=CHC(Me)=CH_2)$ (17). Preparation of this $\eta^4-trans$ -diene tungsten complex was accomplished by using a modified version of the previously published procedure and employing isoprene as the trapping agent.⁵⁵ Previous research in this group has shown that the likelihood of forming the *cis*-isomer was unlikely, because similar *cis*-diene complexes that had been prepared spontaneously isomerized to the thermodynamically more stable *trans* form.^{56–58} In a thick-walled bomb, $Cp^*W(NO)(CH_2SiMe_3)_2$ ⁵⁹ (401 mg, 0.77 mmol) was dissolved in pentane (60 mL), and isoprene (3 mL, 30 mmol) was syringed into the reaction vessel. The resulting mixture was frozen using a liquid N_2 bath, and H_2 gas (14 psig) was then introduced. The contents of the bomb were allowed to warm to room temperature and react while being stirred overnight. After 16 h, the final mixture was concentrated and cooled to obtain yellow crystals of **17** (20 mg, 6%).

17: IR (Nujol, cm^{-1}) 1560 (w, ν_{NO}). MS (LREI, m/z , probe temperature 120 $^{\circ}C$) 417 [P^+ , ^{184}W]. 1H NMR (400 MHz, C_6D_6) δ

(55) Debad, J. D.; Legzdins, P.; Young, M. A. *J. Am. Chem. Soc.* **1993**, *115*, 2051.

(56) Hunter, A. D.; Legzdins, P.; Nurse, C. R. *J. Am. Chem. Soc.* **1985**, *107*, 1791.

(57) Hunter, A. D.; Legzdins, P.; Nurse, C. R.; Einstein, F. W. B.; Willis, A. C.; Bursten, B. E.; Gatter, M. J. *J. Am. Chem. Soc.* **1986**, *108*, 3843.

(58) Christensen, N. J.; Hunter, A. D.; Legzdins, P. *Organometallics* **1989**, *8*, 930.

(59) Legzdins, P.; Rettig, S. J.; Sanchez, L. *Organometallics* **1988**, *7*, 2394.

0.95 (dd, $^2J_{\text{HH}} = 3.91$, $^4J_{\text{HH}} = 0.98$, 1H, C=CH₂), 1.11 (m, 1H, CH), 1.64 (s, 15H, C₅Me₅), 2.05 (s, 3H, CMe), 2.35 (m, 1H, CH=CH₂), 3.15 (dd, $^2J_{\text{HH}} = 4.16$, $^3J_{\text{HH}} = 13.94$, 1H, CH=CH₂), 3.29 (d, $^2J_{\text{HH}} = 3.67$, 1H, C=CH₂). $^{13}\text{C}\{^1\text{H}\}$ NMR (125 MHz, C₆D₆) δ 10.2 (C₅Me₅), 18.5 (CMe), 50.4 (CH=CH₂), 55.2 (C=CH₂), 80.3 (CH), 103.9 (C(Me)=CH₂), 110.2 (C₅Me₅). Sel NOE (400 MHz, C₆D₆) δ irradi. at 2.05, NOE at 3.15 and 3.29, irradi. at 1.64, NOE at 0.95, 1.11, 2.35, and 3.29. Anal. Calcd for C₁₅H₂₃NOW: C, 43.18; H, 5.56; N, 3.36. Found: C, 43.26; H, 5.39; N, 3.34.

Thermolyses of 17 in Benzene-*d*₆ and Cyclohexene. Thermolyses of complex **17** were effected in benzene-*d*₆ and cyclohexene at 50 °C for 6 h to test its thermal stability. After this time, ^1H NMR spectroscopic data (C₆D₆) indicated that no reaction had occurred.

Cp*W(NO)(η^3 -CH₂C(CHCH=CHC₃H₆)CMe₂)(H) (18) and Cp*W(NO)(η^3 -CH₂CHC)(Me)CH₂C₆H₄(C₄H₈)C₆H (19). Complexes **18** and **19** were formed by the thermolysis of **1** (106 mg, 0.22 mmol) in cyclohexene. The volatiles were removed under high vacuum for 1 h, the resulting residue was dissolved in Et₂O, and this solution was transferred to the top of an alumina(I) column (0.5 × 1 cm) and eluted with Et₂O. The yellow/orange eluate thus obtained was again taken to dryness under high vacuum. The residue was recrystallized from a minimal amount of pentane to obtain **18** as a red amorphous solid (19 mg, 35%) and **19** as yellow microcrystals (21 mg, 39%) that could be separated manually.

18: IR (cm⁻¹) 1558 (s, ν_{NO}), 1912 (w, ν_{WH}). MS (LREI, *m/z*, probe temperature 120 °C) 499 [P⁺, ^{184}W]. ^1H NMR (400 MHz, C₆D₆) δ -0.40 (s, $^1J_{\text{WH}} = 131$, 1H, WH), 0.88 (br m, 1H, CH₂C(=CMe₂)), 1.01 (d, $^3J_{\text{WH}} = 1.1$, 3H, =CMe₂), 1.56 (obs, 1H, C₃H₆), 1.76 (s, 15H, C₅Me₅), 1.75 (obs, 1H, C₃H₆), 1.86 (obs, 3H, C₃H₆), 2.01 (br s, 1H, C₃H₆), 2.51 (d, $^3J_{\text{WH}} = 2.5$, 3H, =CMe₂), 3.25 (m, 1H, CH₂C(=CMe₂)), 3.61 (br s, CH(HC=CH)), 5.91 (m, 1H, HC=CH), 6.27 (m, 1H, HC=CH). $^{13}\text{C}\{^1\text{H}\}$ NMR (100 MHz, C₆D₆) δ 10.6 (C₅Me₅), 21.0 (C₃H₆), 25.7 (C₃H₆), 26.5 (Me), 27.3 (Me), 30.9 (C₃H₆), 39.8 (CH(HC=CH)), 45.8 (CH₂C(=CMe₂)), 81.9 (=CMe₂), 105.1 (C₅Me₅), 127.1 (CH₂C(=CMe₂)), 129.2 (HC=CH), 130.1 (HC=CH). Anal. Calcd for C₂₁H₃₃NOW: C, 50.51; H, 6.66; N, 2.80. Found: C, 50.63; H, 6.92; N, 2.83.

19: IR (cm⁻¹) 1559 (s, ν_{NO}). MS (LREI, *m/z*, probe temperature 100 °C) 499 [P⁺, ^{184}W]. ^1H NMR (400 MHz, C₆D₆) δ 1.20 (m, 1H, C₄H₈), 1.23 (m, 1H, C₆H), 1.31 (m, 1H, η^3 -CH₂CHC), 1.38 (obs, 1H, C₄H₈), 1.54 (s, 15H, C₅Me₅), 1.65 (obs, 1H, C₄H₈), 1.73 (obs, 1H, C₆H), 1.76 (obs, 1H, C₄H₈), 1.79 (obs, 1H, C₄H₈), 1.82 (m, 1H, C₄H₈), 1.96 (obs, 1H, CH₂C₆), 2.00 (obs, 1H, η^3 -CH₂CHC), 2.08 (s, 3H, Me), 2.25 (m, 1H, C₄H₈), 2.42 (m, 1H, C₄H₈), 2.44 (m, 1H, CH₂C₆), 3.40 (m, 1H, η^3 -CH₂CHC). $^{13}\text{C}\{^1\text{H}\}$ NMR (100 MHz, C₆D₆) δ 9.7 (C₅Me₅), 21.8 (C₄H₈), 24.6 (Me), 32.7 (η^3 -CH₂CHC), 33.1 (C₄H₈), 33.8 (C₄H₈), 34.1 (C₄H₈), 35.4 (CH₂C₆), 42.2 (C₆), 57.6 (C₆), 93.0 (η^3 -CH₂CHC), 104.8 (C₅Me₅), 139.2 (η^3 -CH₂CHC). Anal. Calcd for C₂₁H₃₃NOW: C, 50.51; H, 6.66; N, 2.80. Found: C, 50.74; H, 6.54; N, 2.79.

Cp*W(NO)(PMe₃)(η^2 -H₂C=C=CMe₂) (20). Complex **20** was prepared by the thermolysis of **1** (67 mg, 0.14 mmol) in neat trimethylphosphine. The final residue was triturated with hexanes (2 × 10 mL), the solvent was removed, and the solid was dried for 1 h under high vacuum. Hexane extracts of this solid were transferred to the top of an alumina(I) column (0.5 × 3 cm) and were eluted with Et₂O to obtain a yellow eluate. The solvent was once again removed from the eluate in vacuo, and the final residue was recrystallized from a 3:1 pentane/Et₂O solvent mix to obtain complex **20** as yellow blocks (16 mg, 24%).

20: IR (cm⁻¹) 1541 (s, ν_{NO}). MS (LREI, *m/z*, probe temperature 120 °C) 493 [P⁺, ^{184}W]. ^1H NMR (400 MHz, C₆D₆) δ 0.67 (d, $^2J_{\text{HH}} = 7.31$, 1H, allene CH₂), 1.27 (d, $^2J_{\text{HP}} = 8.8$, 9H, PMe₃), 1.67 (s, 15H, C₅Me₅), 1.78 (s, 3H, allene Me), 1.97 (br s, 1H, allene CH₂), 2.44 (s, 3H, allene Me). $^{13}\text{C}\{^1\text{H}\}$ NMR (100 MHz, C₆D₆) δ 7.7 (allene CH₂), 10.4 (C₅Me₅), 17.3 (d, $^2J_{\text{CP}} = 31$, PMe₃), 25.9 (allene Me), 31.9 (allene Me), 104.6 (C₅Me₅), 165.7 (=C=CH₂). $^{31}\text{P}\{^1\text{H}\}$ NMR (121 MHz,

C₆D₆) δ -21.4 (s, $^1J_{\text{PW}} = 345$, PMe₃). Sel NOE (400 MHz, C₆D₆) δ irradi. at 0.67, NOE at 1.67, 1.97, and 2.44, irradi. at 1.78, NOE at 1.27 and 2.44. Anal. Calcd for C₁₈H₃₂NOPW: C, 43.83; H, 6.54; N, 2.84. Found: C, 43.65; H, 6.53; N, 2.97.

Cp*W(NO)(η^3 -1,1,2-Me₃C₃H₂)(η^1 -3,3-Me₂C₃H₃) (21). Complex **21** was prepared by the thermolysis of **1** (66 mg, 0.13 mmol) in 2,3-dimethyl-2-butene. The resulting residue was a bright orange/red oil which was triturated with hexanes (2 × 10 mL) to obtain red specks among the oil upon removal of the hexanes in vacuo. The residue was dissolved in Et₂O, and the solution was eluted through an alumina(I) column (0.5 × 3 cm). The solvent was then removed from the eluate, and orange blocks of **21** were isolated by recrystallization of the residue from pentane (26 mg, 38%).

21: IR (cm⁻¹) 1577 (s, ν_{NO}). MS (LREI, *m/z*, probe temperature 120 °C) 501 [P⁺, ^{184}W]. ^1H NMR (400 MHz, C₆D₆) δ 0.70 (s, 3H, η^3 -allyl Me), 1.07 (d, $^2J_{\text{HH}} = 4.6$, 1H, η^3 -allyl CH₂), 1.33 (s, 3H, η^3 -allyl Me), 1.56 (obs, 1H, η^1 -allyl CH₂), 1.59 (s, 15H, C₅Me₅), 1.96 (s, 3H, η^1 -allyl Me), 1.97 (obs, 1H, η^1 -allyl CH₂), 1.98 (s, 3H, η^1 -allyl Me), 2.19 (s, 3H, η^3 -allyl CMe), 2.48 (d, $^2J_{\text{HH}} = 4.6$, 1H, η^3 -allyl CH₂), 5.82 (t, $^3J_{\text{HH}} = 7.3$, 1H, η^1 -allyl CH). $^{13}\text{C}\{^1\text{H}\}$ NMR (100 MHz, C₆D₆) δ 9.9 (C₅Me₅), 18.6 (η^1 -allyl Me), 18.6 (η^1 -allyl CH₂), 22.6 (η^3 -allyl Me), 22.6 (η^3 -allyl Me), 22.8 (η^3 -allyl Me), 26.0 (η^1 -allyl Me), 44.8 (η^3 -allyl CH₂), 106.9 (C₅Me₅), 133.3 (η^1 -allyl-CH). Sel NOE (400 MHz, C₆D₆) δ irradi. at 1.59, NOE at 0.70 and 1.07. Anal. Calcd for C₂₁H₃₅NOW: C, 50.31; H, 7.04; N, 2.79. Found: C, 50.58; H, 7.20; N, 2.89.

Cp*W(NO)(η^3 -C₆H₅)(H) (22) and Cp*W(NO)(η^3 -C₇H₁₁)(H) (23a,b). Complex **22** was formed via thermolysis of **1** (50 mg, 0.10 mmol) in cyclohexane, and complexes **23a,b** were formed via the thermolysis of **1** (80 mg, 0.16 mmol) in methylcyclohexane. The reaction mixtures at the end of the 6-h periods were a dark orange/brown color, and the residues formed upon removal of the solvent were brown oils. The residues were triturated with hexanes (2 × 10 mL) which were dried under high vacuum for approximately 1 h to obtain mixtures of dark specks interspersed in brown oils. These mixtures were then redissolved in 1:3 Et₂O/hexanes solvent mixtures, and the resulting solutions were eluted through alumina(I) columns (0.5 × 3 cm) to obtain yellow eluates. The solvent was once again removed in vacuo, and the final residues were recrystallized from 3:1 pentane/Et₂O solvent mixtures to obtain complexes **23a,b** as yellow microcrystals (3.5 mg, 5%), and complex **22** as yellow blocks (14 mg, 32%). Complexes **23a,b** were identified by comparison of their ^1H NMR spectra to those previously reported.²⁰

22: IR (cm⁻¹) 1568 (s, ν_{NO}), 1898 (m, ν_{WH}). MS (LREI, *m/z*, probe temperature 120 °C) 431 [P⁺, ^{184}W]. ^1H NMR (500 MHz, C₆D₆) δ -0.57 (s, $^1J_{\text{WH}} = 132$, 1H, WH), 1.16 (m, 1H, cyclohexenyl C₄H₂), 1.42 (m, 1H, cyclohexenyl C₆H₂), 1.69 (s, 15H, C₅Me₅), 2.46 (m, 1H, cyclohexenyl C₆H₂), 2.58 (m, 1H, cyclohexenyl C₆H₂), 2.62 (m, 2H, cyclohexenyl C₆H₂), 2.75 (m, 1H, allyl C₆H), 3.59 (m, 1H, allyl C₇H), 5.30 (m, 1H, allyl C₇H). $^{13}\text{C}\{^1\text{H}\}$ NMR (125 MHz, C₆D₆) δ 10.4 (C₅Me₅), 19.9 (cyclohexenyl C₄H₂), 26.6 (cyclohexenyl C₆H₂), 28.7 (cyclohexenyl C₆H₂), 61.8 (allyl C₇H₂), 73.4 (allyl C₇H), 93.2 (allyl C₇H₂), 103.9 (C₅Me₅). Anal. Calcd for C₁₆H₂₅NOSiW: C, 44.56; H, 5.84; N, 3.25. Found: C, 44.40; H, 5.76; N, 3.24.

Kinetic Studies. A J. Young NMR tube was charged with **1** (10 mg, 0.020 mmol), benzene-*d*₆ (0.8 mL), and hexamethyldisilane (1 mg, 0.007 mmol) as an inert internal standard, and the contents were mixed thoroughly. The thermolysis of **1** was monitored by ^1H NMR spectroscopy at 323.0 K with the number of scans set to one. The loss of starting material versus time was determined by the integration of the neopentyl CMe₃ signal versus the hexamethyldisilane signal, except for the $t = 0$ value which was extrapolated from the plot of starting material loss versus time. The first-order rate constant for the decomposition of **1** was determined from the plot of $\ln(I(t)/I(0))$ versus time. After 4.5 h, the sample was removed from the probe, and the crystalline product **4a-c-d**₆ was analyzed by NMR and MS spectroscopic techniques.

Table 1. X-ray Crystallographic Data for Complexes **2**, **3**, **4**, **18**, **19**, **20**, and **21**

	2	3	4	18	19	20	21
Crystal Data							
empirical formula	C ₁₉ H ₃₅ NOWSi	C ₂₄ H ₃₅ NOW	C ₂₁ H ₂₉ NOW	C ₂₁ H ₃₃ NOW	C ₂₁ H ₃₃ NOW	C ₁₈ H ₃₂ NOPW	C ₂₁ H ₃₅ NOW
cryst habit, color	platelet, orange	block, orange	prism, yellow	block, yellow	block, yellow	chip, yellow	prism, yellow
cryst size (mm)	0.30 × 0.15 × 0.08	0.40 × 0.30 × 0.15	0.30 × 0.20 × 0.20	0.90 × 0.20 × 0.10	0.30 × 0.25 × 0.05	0.25 × 0.20 × 0.10	0.45 × 0.35 × 0.20
cryst syst	monoclinic	orthorhombic	monoclinic	orthorhombic	orthorhombic	monoclinic	monoclinic
space group	C2/c	Pbca	P2 ₁ /c	P2 ₁ 2 ₁ 2 ₁	Pbca	P2 ₁ /c	P2 ₁ /n
vol (Å ³)	4228.4(3)	4456.2(3)	1949.6(1)	2013.0(3)	3908.5(5)	1969.10(18)	2055.5(3)
a (Å)	15.3944(6)	14.2207(7)	12.8869(3)	8.2431(7)	14.8888(10)	9.1458(5)	9.1734(7)
b (Å)	8.4977(3)	15.9939(7)	9.0219(3)	9.2094(9)	14.7065(9)	13.6500(7)	16.9621(11)
c (Å)	32.326(1)	19.5926(9)	16.7835(7)	26.517(3)	17.8503(12)	15.9576(9)	13.2647(10)
α (deg)	90	90	90	90	90	90	90
β (deg)	90.753(3)	90	92.439(2)	90	90	98.724(3)	95.201(4)
γ (deg)	90	90	90	90	90	90	90
Z	8	8	4	4	8	4	4
density (calc) (Mg/m ³)	1.500	1.602	1.687	1.648	1.697	1.664	1.62
abs coeff (cm ⁻¹)	54.73	52.03	59.39	5.75	5.92	59.50	58.05
F ₀₀₀	1904.00	2144.00	976.00	992	1984	976	1000
Data Collection and Refinement							
measd reflns: total	12 879	41 082	13 123	4239	4347	4136	4496
measd reflns: unique	4410	5645	4484	3863	3155	3358	3684
final R indices ^a	R1 = 0.036, wR2 = 0.071	R1 = 0.031, wR2 = 0.038	R1 = 0.038, wR2 = 0.066	R1 = 0.0246, wR2 = 0.049	R1 = 0.0331, wR2 = 0.0825	R1 = 0.0281, wR2 = 0.067	R1 = 0.0311, wR2 = 0.075
GOF on F ² ^b	1.60	0.80	1.07	0.882	0.888	0.947	0.985
largest diff. peak and hole (e Å ⁻³)	2.01 and -1.75	3.30 and -2.01	1.08 and -1.64	0.92 and -1.02	2.985 and -3.000	1.580 and -2.497	3.379 and -1.460

^a R1 on F = $\sum(|F_o| - |F_c|)/\sum|F_o|$; wR2 = $[(\sum(F_o^2 - F_c^2)^2)/\sum w(F_o^2)^2]^{1/2}$; w = $[\sigma^2 F_o^2]^{-1}$. ^b GOF = $[\sum(w(|F_o| - |F_c|)^2)/\text{degrees of freedom}]^{1/2}$.

X-ray Crystallography. Data collection for each compound was carried out at -100 ± 1 °C on a Rigaku/ADSC CCD diffractometer using graphite-monochromated Mo K α radiation.

Data for **2** were collected to a maximum 2θ value of 55.9° in 0.5° oscillations with 27.0 s exposures. The structure was solved by direct methods⁶⁰ and expanded using Fourier techniques.⁶¹ All non-hydrogen atoms were refined anisotropically; hydrogen atoms H11a, H11b, and H12 were refined isotropically, and all other hydrogen atoms were included in fixed positions. The final cycle of full-matrix least-squares analysis was based on 4156 observed reflections and 221 variable parameters.

Data for **3** were collected to a maximum 2θ value of 55.7° in 0.5° oscillations with 20.0 s exposures. The structure was solved by direct methods⁶⁰ and expanded using Fourier techniques.⁶¹ All non-hydrogen atoms were refined anisotropically; hydrogen atoms H16, H17, H27, H28, and H29 were refined isotropically, and all other hydrogen atoms were included in fixed positions. The final cycle of full-matrix least-squares analysis was based on 5120 observed reflections and 264 variable parameters.

Data for **4** were collected to a maximum 2θ value of 57.5° in 0.5° oscillations with 12.0 s exposures. The structure was solved by direct methods⁶⁰ and expanded using Fourier techniques.⁶¹ All non-hydrogen atoms were refined anisotropically; hydrogen atoms H6, H7, and H8 were refined isotropically, and all other hydrogen atoms were included in fixed positions. The final cycle of full-matrix least-squares analysis was based on 4264 observed reflections and 229 variable parameters.

Data for **18** were collected to a maximum 2θ value of 55.7° in 0.5° oscillations with 35.0 s exposures. The structure was solved by direct methods⁶² and expanded using Fourier techniques.⁶¹ All non-hydrogen atoms were refined anisotropically; hydrogen atoms H11a, H11b, and H22 were refined isotropically, and all other hydrogen atoms were

included in fixed positions. The final cycle of full-matrix least-squares analysis was based on 4239 observed reflections and 236 variable parameters.

Data for **19** were collected to a maximum 2θ value of 55.8° in 0.5° oscillations with 23.0 s exposures. The structure was solved by direct methods⁶² and expanded using Fourier techniques.⁶¹ All non-hydrogen atoms were refined anisotropically; hydrogen atoms H11a, H11b, H12a, H16a, and H21a were refined isotropically, and all other hydrogen atoms were included in fixed positions. The final cycle of full-matrix least-squares analysis was based on 4347 observed reflections and 243 variable parameters.

Data for **20** were collected to a maximum 2θ value of 55.8° in 0.5° oscillations with 20.0 s exposures. The structure was solved by direct methods⁶² and expanded using Fourier techniques.⁶¹ All non-hydrogen atoms were refined anisotropically; hydrogen atoms H1 and H2 were refined isotropically, and all other hydrogen atoms were included in fixed positions. The final cycle of full-matrix least-squares analysis was based on 4135 observed reflections and 217 variable parameters.

Data for **21** were collected to a maximum 2θ value of 55.7° in 0.5° oscillations with 20.0 s exposures. The structure was solved by direct methods⁶² and expanded using Fourier techniques.⁶¹ All non-hydrogen atoms were refined anisotropically; hydrogen atoms H1, H2, H3, H4, and H5 were refined isotropically, and all other hydrogen atoms were included in fixed positions. The final cycle of full-matrix least-squares analysis was based on 4496 observed reflections and 247 variable parameters.

For each structure, neutral-atom scattering factors were taken from Cromer and Waber.⁶³ Anomalous dispersion effects were included in F_{calc} ; the values for $\Delta f'$ and $\Delta f''$ were those of Creagh and McAuley.⁶⁵ The values for mass attenuation coefficients are those of Creagh and Hubbell.⁶⁶ All calculations were performed using the CrystalClear software package of Rigaku/MS, the teXsan crystallographic

(60) SIR97: Altomare, A.; Burla, M. C.; Cammelli, G.; Casciarano, M.; Giacovazzo, C.; Guagliardi, A.; Moliterni, A. G. G.; Polidori, G.; Spagna, A. *J. Appl. Crystallogr.* **1999**, *32*, 115–119.

(61) PATTY: Beurskens, P. T.; Admirals, G.; Beurskens, G.; Bosman, W. P.; Garcia-Granda, S.; Gould, R. O.; Smits, J. M. M.; Smykalla, C. University of Nijmegen, The Netherlands, 1992.

(62) SIR92: Altomare, A.; Casciarano, M.; Giacovazzo, C.; Guagliardi, A. *J. Appl. Crystallogr.* **1993**, *26*, 343.

(63) Cromer, D. T.; Waber, J. T. *International Tables for X-ray Crystallography*; Kynoch Press: Birmingham, 1974; Vol. IV.

(64) Ibers, J. A.; Hamilton, W. C. *Acta Crystallogr.* **1964**, *17*, 781–782.

(65) Creagh, D. C.; McAuley, W. J. *International Tables for X-ray Crystallography*; Kluwer Academic Publishers: Boston, 1992; Vol. C.

(66) Creagh, D. C.; Hubbell, J. H. *International Tables for X-ray Crystallography*; Kluwer Academic Publishers: Boston, 1992; Vol. C.

software package of Molecular Structure Corp.,⁶⁸ or Shelxl-97.⁶⁹ X-ray crystallographic data for all seven structures are presented in Table 1, and full details of all crystallographic analyses are provided in the Supporting Information.

Acknowledgment. We are grateful to the Natural Sciences and Engineering Research Council of Canada for support of this work in the form of grants to P.L. and postgraduate

scholarships to C.S.A. and T.W.H. We also thank Ms. N. Thompson for assistance with the statistical analyses and Dr. C. B. Pamplin for technical assistance. P.L. is a Canada Council Killam Research Fellow.

Supporting Information Available: Kinetic data for the thermal decomposition of **1** in benzene-*d*₆ at 50 °C (PDF) and full details of crystallographic (CIF) analyses of complexes **2**, **3**, **4**, **18**, **19**, **20**, and **21**. This material is available free of charge via the Internet at <http://pubs.acs.org>.

JA037076Q

- (67) CrystalClear: Version 1.3.5b20; Molecular Structure Corp.: The Woodlands, TX, 2002.
(68) teXsan; Molecular Structure Corp.: The Woodlands, TX, 1985 and 1992.
(69) SHELXL97; Sheldrick, G. M. University of Göttingen: Germany, 1997.